A THEORETICAL ANALYSIS OF TWO DIMENSIONAL CASCADE FLOW WITH APPLICATION ON AN AXIAL FLOW PUMP

Thesis by

Richard L. Robinson

In Partial Fulfillment of the Requirements

For the Degree of

Mechanical Engineer

California Institute of Technology

Pasadena, California

1950

ACKNOWLEDGMENTS

My most sincere appreciation goes to Professor W. Duncan Rannie for giving generously of his free time and helpful advice.

Thanks, also, to my loving wife, Jessie C. Robinson, for spending many patient hours going over this paper for grammatical mistakes as well as typing it in the final form.

SUMMARY

This paper presents a method for solving the two dimensional cascade flow problem. This method of solution utilizes the slopes of the airfoil instead of the airfoil shape as has been done in most previous solutions. The value of this step is the numerical accuracy gained in solving for the velocity distribution directly, without the differentiation required in other methods.

An application of this method is made to a three bladed axial flow pump using a standard NACA 4400 series airfoil for the blade shapes.

CONTENTS

NOTATIONS OFTEN USED

A_n	constant used in the transformation series.
a	radius of the circle in the ζ -plane.
B_n	constant used in the transformation series.
b	one-half chord length of the flat plate.
C_ν	constant used in determination of the cosine part in the series approximation.
C_L	coefficient of lift for a cascade airfoil.
d	distance between airfoils of the cascade measured along the direction of the cascade angle.
F	velocity potential function for the cascade.
N	number of divisions into which the circle of the ζ -plane is divided for the transformation series approximation.
q	local velocity at any point on a cascade airfoil.
R	pump section radius except as noted.
S	gap/chord ratio for the cascade.
S_ν	constant used in determination of the sine part in the series approximation.
u	horizontal component of free stream velocity.
V	$=u+iv$ free stream velocity in the cascade plane.
Ve	velocity leaving the cascade of airfoils.
Vi	velocity entering the cascade of airfoils.
v	vertical component of free stream velocity.
X	horizontal component in the Z -plane.
y	vertical component in the Z -plane.
Z	$=X+iy$ cascade plane.

α angle of attack of V with respect to the chord of the airfoil.

β cascade angle measured between the y -axis and a line of the cascade drawn through the leading edges of the airfoils in the cascade.

Γ circulation about an airfoil in the cascade.

γ_e angle of velocity leaving the cascade measured with reference to a line drawn through the trailing edges of the airfoils in the cascade.

γ_i angle of velocity entering the cascade measured with reference to a line drawn through the leading edges of the airfoils in the cascade.

Δ indicates a perturbation function in the transformation. $[\Delta x(\phi)]$

δ constant used in the transformation of the x-component of the cascade airfoil.

ϵ constant used in the transformation of the x-component of the cascade airfoil.

ζ $= \xi + i\eta$ plane of the circle into which the cascade is transformed.

η vertical component in the ζ -plane.

θ $= \frac{2\pi}{N}$ angular sectors into which the circle is divided to determine the transformation series approximation.

ξ horizontal component in the ζ -plane.

ϕ angular notation for polar coordinates in the ζ -plane.

ϕ_L angle in the ζ -plane corresponding to the leading edge of the airfoil in the z -plane.

ϕ_T angle in the ζ -plane corresponding to the trailing edge of the airfoil in the z -plane.

χ constant in the flat plate cascade transformation determined by the cascade dimensions.

ψ $e^{-\gamma} = \chi$ constant used to replace χ for the final transformation.

Subscripts

j 0 to N-1. Used to designate the values of ϕ when the circle in the ζ -plane is divided into N parts.

n 0 to ∞. Used to designate the coefficients of the series summation.

μ 1 to $\frac{N-1}{2}$. Used to designate the coefficients in the series approximations.

ν 0 to $\frac{N-1}{2}$. Used to designate the values used in determining the coefficients for the series approximation.

Superscripts

$'$ prime indicates a first derivative.

$''$ double prime indicates a second derivative.

PART I

INTRODUCTION

This paper presents a method for solving the two dimensional flow problem in a cascade of airfoils. The two dimensional problem must be considered when the airfoils of the cascade are so far apart that the form of the flow cannot be determined from the direction and the cross-sectional area of the passage between the airfoils. This is the situation that exists in most pumps and compressors where the airfoils do not have a very appreciable overlap.

We speak of pumps and compressors as being two dimensional flow problems. This is true if we make the assumption that the flow proceeds through the vane system of the pump along concentric cylindrical surfaces. This assumption will not be too far off when the pump is operating within the vicinity of its best efficiency point because the flow pattern approximates that of an ideal fluid. The two dimensional picture is then obtained by unrolling the concentric cylindrical surface.

In making a theoretical analysis of the flow we can consider the vane system stationary. This can be done due to the fact that the relative flow through such a moving system along a constant radius obeys Bernoulli's equation in the same manner as for the absolute flow through the system at rest.

The final assumption to be made in connection with the treatment presented by this paper is a frictionless fluid. This assumption does much to simplify the calculations and does not throw the results very far off as shown by experience with other problems of a similar nature.

The pump to which the two-dimensional solution of the flow pattern was applied is a Peerless 10-PL propellor pump. This pump was used because it will soon be tested in the Hydrodynamics Laboratory at the California Institute of Technology and will thus offer a means of checking the accuracy of the method.

Previously two lines of attack have been employed for the general solution of the two-dimensional flow problem for a cascade. The first seeks to reduce the unknown flow through the cascade to the known flow around a circle by a group of conformal transformations. The second attempts to modify the flow about an individual airfoil by evaluating an interference function arising from the presence of the other airfoils in the cascade. The interference method is thoroughly described in the paper of Katzoff, Finn, and Laurence (1). Advantages are claimed for this method particularly in solving the inverse problem, that is, finding the airfoil in a cascade for a given velocity distribution.

One of the earliest papers on a method for the exact solution of flow past an arbitrary airfoil cascade is that

of Weinig (2). He used a transformation that takes a cascade of flat plates to a circle. The use of this transformation on a given cascade yields a shape that more or less resembles a circle. This shape is then modified to an exact circle by a method similar to that of Theordorsen and Garrick (3). This method is quite lengthy and as a result does not prove to be very practical. This principle is also similar to that used by Garrick (4) and also Mutterperl (5). The method of Howell's (6) is somewhat different from the above methods. The difference lies in the fact that two transformations are used to change the cascade to a near circle. The first transformation changes the cascade to a single S shaped airfoil and the second transformation changes this single airfoil to a near circle.

Goldstein and Jerison (7) have recently worked out a general solution for the inverse cascade problem by an adaptation of the interference method. Diesendruck (8), using the interference method, has recently solved the flow solution of particular thin blade cascade problems. There are several other approximate solutions for the general cascade and exact solutions for specific cascade shapes that will not be mentioned here.

The numerical work for the general solution of the cascade flow is naturally great, due to the fact that in cascade transformations singularities are located quite

close to the circle into which the cascade is transformed. This means that the solution will not converge too rapidly so that several iterations are necessary to produce the required accuracy. In spite of the labor involved, however, this category is the most valuable due to its generality.

All of the above methods work directly from the airfoil shapes. In this paper a different approach is made in that a method utilizing the slope curves of the airfoil, instead of the airfoil itself, is used to solve the general cascade flow problems. There are two reasons for using this method. First, by solving the problem using the slope curve of an airfoil, a differentiation necessary in the other methods is eliminated in solving for the velocity distribution. This means that errors which enter into the computations are no longer magnified by a differentiation and accuracy should therefore be improved. Secondly, since the accuracy has been improved, the number of iterations necessary to obtain the desired accuracy should be less, or possibly fewer terms may be used in the perturbation summation with the same number of iterations involved.

PART II

THE CASCADE TRANSFORMATION

The purpose of the transformation is to change the complicated two dimensional flow pattern of a cascade of infinite airfoils into the flow pattern around an infinite cylinder which can be readily solved. This is accomplished in the following manner.

The equation (9)

$$Z = \frac{d}{2\pi}\left[e^{-i\beta} \log \frac{a+\chi\zeta}{a-\chi\zeta} + e^{i\beta} \log \frac{\zeta+a\chi}{\zeta-a\chi} \right] \qquad (1)$$

transforms a cascade of straight lines into a circle as shown in Fig. 1. The vortex and source at $\zeta = -a/\chi$ corresponds to $Z = -\infty$ and the vortex and sink at $\zeta = +a/\chi$ corresponds to $Z = +\infty$. This means the flow from the source in the ζ- plane as shown in Fig. 1 is equivalent to rectilinear flow in the Z -plane parallel to the X-axis, while the flow from the vortexes is equivalent to rectilinear flow parallel to the Y-axis, both flows being in the positive direction. Thus, the resultant flow at the cascade airfoil is the vector sum of these two flow velocities. In the Y-direction a point half way between two consecutive straight lines is at infinity in the ζ-plane, being at positive infinity with respect to the lower straight line and negative infinity with respect to the upper straight line.

For convenience, let us make the circle one of unit

radius and replace χ by $e^{-\psi}$ thus obtaining the following equation:

$$Z = \frac{d}{2\pi}\left[e^{-i\beta}\log\frac{e^{+\psi}+\zeta}{e^{+\psi}-\zeta} + e^{i\beta}\log\frac{\zeta+e^{-\psi}}{\zeta-e^{-\psi}}\right] \qquad (2)$$

The parameter ψ is related to the chord-gap ratio, and this relationship is established in the following manner. We know that at the edges of the straight line airfoils, we have

$$\frac{dZ}{d\zeta} = e^{-i\beta}\left[\frac{1}{e^{+\psi}+\zeta} + \frac{1}{e^{+\psi}-\zeta}\right] + e^{i\beta}\left[\frac{1}{\zeta+e^{-\psi}} - \frac{1}{\zeta-e^{-\psi}}\right] = 0 \qquad (3)$$

Since $\zeta = e^{i\phi}$ on the circle which transforms to the straight line, we can simplify the above equation obtaining (9)

$$\tan\phi = \frac{e^{2\psi}-1}{e^{2\psi}+1}\tan\beta \qquad (4)$$

Denoting the two roots by ϕ_T for the trailing edge and ϕ_L for the leading edge of the straight line and noting $\phi_L = \pi + \phi_T$, we can obtain the chord length. This is done by substituting the values of ϕ on the circle for the leading and trailing edges of the straight line into the expression for Z and taking the difference of the two values. In this manner, we obtain (9)

$$2b = \frac{2d}{\pi}\left[\sin\beta\tan^{-1}\frac{2\sin\beta}{\sqrt{2\cosh 2\psi + 2\cos 2\beta}} - \cos\beta\log\frac{2\sinh\psi}{\sqrt{2\cosh 2\psi + 2\cos 2\beta + 2\cos\beta}}\right] \qquad (5)$$

Knowing b, d, and β, we can solve this equation for ψ and thus we have determined the relationship between the

chord-gap ratio and Ψ .

Let us introduce the following changes in the transformation. First, let the chord length of the straight line equal unity. The distance between the airfoils becomes $\frac{d}{2b} = S$. By a simple translation, we obtain the following transformation

$$Z = \frac{1}{2} + \frac{S}{2\pi}\left[e^{-i\beta}\log\frac{e^{+\Psi}+\zeta}{e^{+\Psi}-\zeta} + e^{i\beta}\log\frac{\zeta+e^{-\Psi}}{\zeta-e^{-\Psi}}\right] \qquad (6)$$

This makes the transformation of the cascade of straight lines as shown in Fig. 2. If a curve representing an airfoil with both thickness and camber is drawn in the Z-plane in place of the straight line airfoil, the transformation does not go into a circle, but the variation from the circle will not be very great if thickness and camber are small as is the case in the typical airfoil. In order to eliminate the variations in the circle caused by thickness and camber, perturbations of the form

$$\sum_{0}^{\infty}\frac{A_n + i\,B_n}{\zeta^n}$$

are added to equation 6 to change the transformation again into a perfect circle. A perturbation of this type will also change the x values as well as the y values of the equation. These changes are as follows:

$$\Delta X(\phi) = \sum_{n=1}^{\infty}\left[A_n\cos(n\phi) + B_n\sin(n\phi)\right]$$
$$\Delta Y(\phi) = B_0 + \sum_{n=1}^{\infty}\left[B_n\cos(n\phi) - A_n\sin(n\phi)\right] \qquad (7)$$

In order to keep the chord length of the airfoil at unity, a factor ϵ must be introduced to account for changes in length of the transformation caused by $\Delta x(\phi)$ as well as a constant δ to account for any translation of the airfoil caused by $\Delta x(\phi)$. The transformation now has the following form:

$$Z = (1+\epsilon) f(\phi) + \sum_{n=0}^{\infty} \frac{A_n + i B_n}{\zeta^n} + \delta \qquad (8)$$

where $f(\phi) = \frac{1}{2} + \frac{s}{2\pi}\left[e^{-i\beta} \log \frac{e^{+\psi} + \zeta}{e^{+\psi} - \zeta} + e^{i\beta} \log \frac{\zeta + e^{-\psi}}{\zeta - e^{-\psi}} \right]$

and $\zeta = e^{i\phi}$ on the unit circle. Rewriting the equation in x and y, we have

$$\begin{aligned} x &= (1+\epsilon) f(\phi) + \Delta x(\phi) + \delta \\ y &= \Delta y(\phi) \end{aligned} \qquad (9)$$

This will give the transformation as shown in Fig. 3.

At the leading and trailing edges of the airfoil

$$\frac{dx}{d\phi} = (1+\epsilon) f'(\phi) + \Delta x'(\phi) = 0$$

where $f'(\phi) = \frac{d[f(\phi)]}{d\phi}$ and $\Delta x'(\phi) = \frac{d[\Delta x(\phi)]}{d\phi}$

Therefore

$$(1+\epsilon) f'(\phi) = -\Delta x'(\phi) \qquad (10)$$

where $\phi = \phi_T$ or ϕ_L

Knowing ϕ_T and ϕ_L , ϵ can be determined by dividing the change in length due to the perturbations by the length without the perturbations. Thus

$$\epsilon = \frac{1 - f(\phi_T) + f(\phi_L) - \Delta X(\phi_T) + \Delta X(\phi_L)}{f(\phi_T) - f(\phi_L)} \qquad (11)$$

is determined from the fact that $x=1$ at ϕ_T.

Therefore $$1 = (1+\epsilon) f(\phi_T) + \Delta X(\phi_T) + \delta$$

and $$\delta = 1 - (1+\epsilon) f(\phi_T) + \Delta X(\phi_T). \qquad (12)$$

ϕ_T and ϕ_L are determined from equation 10 and yet ϕ_T and ϕ_L are necessary to determine ϵ which is a part of equation 10. This must therefore be done by successive approximations. First, make the assumption that $\epsilon = 0$ and determine ϕ_T and ϕ_L, then using these values determine from equation 11. Using the new value of ϵ redetermine ϕ_T and ϕ_L. Repeat this cycle until there is no apparent change in ϵ or ϕ_T and ϕ_L. Once this is done δ can also be determined because ϕ_T and ϵ are now known.

The only thing necessary to complete the transformation is a method of determining the A's and B's of the summation

$$\sum_{n=0}^{\infty} \frac{A_n + i B_n}{\zeta^n}$$

There are many ways of doing this but the following method was used in obtaining the results for this paper.

Divide the circle into an odd number of sectors, the greater the accuracy desired the greater the number of divisions that should be used. Using the straight line transformation as a first approximation, the values of x for the various ϕ_j divisions can be determined. Then from

the shape of the airfoil, the y components can be determined at each of the calculated lengths. Knowing the y_j's and ϕ_j's, the series can now be found. An example of the method used will be worked out for 5 divisions of the circle (see Fig. 4), but the same procedure can be used for any number of odd divisions.

Knowing the y components for the various angles, we write the following equations

$$y_0 = B_0 + B_1 + B_2$$

$$y_1 = B_0 + B_1 \cos\theta + B_2 \cos 2\theta - A_1 \sin\theta - A_2 \sin 2\theta$$

$$y_2 = B_0 + B_1 \cos 2\theta + B_2 \cos 4\theta - A_1 \sin 2\theta - A_2 \sin 4\theta$$

and so on to y_4 where $\phi_1 = \theta$, $\phi_2 = 2\theta$, etc. Noting that $4\theta = -\theta$ and $3\theta = -2\theta$, we can by addition and subtraction of the equations determine the following equations:

$$y_0 = B_0 + B_1 + B_2$$

$$y_1 + y_4 = 2B_0 + 2B_1 \cos\theta + 2B_2 \cos 2\theta$$

$$y_2 + y_3 = 2B_0 + 2B_1 \cos 2\theta + 2B_2 \cos\theta$$

$$y_1 - y_4 = -2A_1 \sin\theta - 2A_2 \sin 2\theta$$

$$y_2 - y_3 = -2A_1 \sin 2\theta - 2A_2 \sin\theta$$

Let $C_0 = y_0$, $C_1 = y_1 + y_4$, $C_2 = y_2 + y_3$, and solving for B_0, B_1, and B_2, we obtain

$$B_0 = \frac{1}{5}(C_0 + C_1 + C_2)$$

$$B_1 = \frac{2}{5}(C_0 + C_1 \cos\theta + C_2 \cos 2\theta)$$

$$B_2 = \frac{2}{5}(C_0 + C_1 \cos 2\theta + C_2 \cos\theta)$$

Similarly, letting $S_1 = y_1 - y_4$ and $S_2 = y_2 - y_3$, we obtain

$$A_1 = \frac{2}{5}(S_1 \sin\theta + S_2 \sin 2\theta)$$

$$A_2 = \frac{2}{5}(S_1 \sin 2\theta + S_2 \sin\theta)$$

Tables listing the solutions of the coefficients for any number of points as solved by this method are given in Stumpff's, "Tafeln Und Aufgaben Zur Harmonischen Analyse Und Periodogrammrechnung" (10). These tables were used in obtaining the results for this paper.

For the transformation,

$$y = B_0 + \sum_{n=1}^{\infty}\left[B_n \cos(n\phi) - A_n \sin(n\phi)\right] \tag{13}$$

and $$\frac{dy}{d\phi} = \sum_{n=1}^{\infty}\left[-n B_n \sin(n\phi) - n A_n \cos(n\phi)\right]$$

We see that if we have a method of obtaining $\frac{dy}{d\phi}$, we can use this to determine the coefficients. Such a method would have several advantages over determining the coefficients from the shape of the airfoil. First, the slopes are used in determining the velocity distribution about the airfoil, and since the solution of the velocity distribution is the primary purpose of the transformation, this gives you the direct solution. Secondly, the errors involved in obtaining the coefficients from y are magnified many times in obtaining $\frac{dy}{d\phi}$ from y, because the coefficients are multiplied by n, so the errors in each coefficient are now n times as large. Going from $\frac{dy}{d\phi}$ to y, however,

any errors made orginally are reduced by an integration instead of magnified.

A method of determining $\frac{dy}{d\phi}$ is as follows. Take the airfoil shape and from this determine $\frac{dy}{dx}$ as a function of x. Since $\frac{dy}{d\phi} = \frac{dx}{d\phi}\,\frac{dy}{dx}$, as a first approximation we use the straight line transformation and obtain x and $\frac{dx}{d\phi}$ for the ϕ_j's into which the circle is divided. Knowing x, $\frac{dy}{dx}$ can be determined from the curves made from the airfoil shape. We now have a first approximation to $\frac{dy}{d\phi}$. Using this we determine the coefficients for the summation, and thus obtain $\Delta X(\phi)$ from equation 7. Knowing $\Delta X(\phi)$, we obtain $\phi_T, \phi_L, \epsilon,$ and δ as described on page 9. This gives the first approximation to the final transformation in the form of equation 9. By using the new transformation to obtain x and $\frac{dx}{d\phi}$, and repeating the procedure given above, a new and better approximation to the final transformation is obtained. This is repeated until very little change is obtained between two successive approximations. With this, we have the final solution for the transformation of a cascade of airfoils to a circle.

We now proceed to the calculation of the flow around the cascade. Writing the potential function for the flow about the circle, for the straight line transformation as shown in Fig. 2, we have (9)

$$F = \frac{VS}{2\pi}\left[e^{-i(\beta+\alpha)}\log\frac{e^{+\psi}+\zeta}{e^{+\psi}-\zeta} + e^{i(\beta+\alpha)}\log\frac{\zeta+e^{-\psi}}{\zeta-e^{-\psi}}\right] + \frac{i\Gamma}{4\pi}\frac{\zeta^2-e^{-2\psi}}{\zeta^2-e^{2\psi}} \qquad (14)$$

By comparison with the final transformation equation, we see that the only change in the velocity potential function is the factor $(1+\epsilon)$, and thus obtain

$$F = \frac{VS(1+\epsilon)}{2\pi}\left[e^{-i(\beta+\alpha)}\log\frac{e^{+\psi}+\zeta}{e^{+\psi}-\zeta} + e^{i(\beta+\alpha)}\log\frac{\zeta+e^{-\psi}}{\zeta-e^{-\psi}}\right] + \frac{i\Gamma(1+\epsilon)}{4\pi}\log\frac{\zeta^2-e^{-2\psi}}{\zeta^2-e^{2\psi}} \qquad (15)$$

This is for a velocity in the $\mathcal{Z}$ -plane of

$$Ve^{-i\alpha} - \frac{i\Gamma}{2S}e^{-i\beta} \qquad \text{at} \quad X = -\infty$$

and

$$Ve^{-i\alpha} + \frac{i\Gamma}{2S}e^{-i\beta} \qquad \text{at} \quad X = +\infty$$

These are determined as follows:

$$\left(\frac{dF}{dz}\right)_{-\infty} = \left(\frac{dF}{d\zeta}\right)_{\zeta=-e^{\psi}}\left(\frac{d\zeta}{dz}\right)_{\zeta=-e^{\psi}} = Ve^{-i\alpha} - \frac{i\Gamma}{2S}e^{-i\beta}$$

The velocity at the airfoil boundary is given in the same manner

$$\left(\frac{dF}{dz}\right)_{\zeta=e^{i\phi}} = \left(\frac{dF}{d\zeta}\right)_{\zeta=e^{i\phi}}\left(\frac{d\zeta}{dz}\right)_{\zeta=e^{i\phi}} = u - iv$$

This can be rewritten in the following way on the airfoil

$$u - iv = \left(\frac{dF}{d\phi}\,\frac{d\phi}{dz}\right)$$

now let $R = \log\dfrac{\zeta^2-e^{-2\psi}}{\zeta^2-e^{2\psi}} = \log\dfrac{e^{2\phi}-e^{-2\psi}}{e^{2\phi}-e^{2\psi}}$

then

$$F = V(1+\epsilon)\, f(\phi) + \frac{i\Gamma(1+\epsilon)}{4\pi} R$$

$$\frac{dF}{d\phi} = V(1+\epsilon)\, f'(\phi) + \frac{i\Gamma(1+\epsilon)}{4\pi}\frac{dR}{d\phi} \qquad \text{and} \qquad \frac{dR}{d\phi} = -\frac{2i\sinh 2\psi}{\cosh 2\psi - \cos 2\phi}$$

$$\frac{dZ}{d\phi} = (1+\epsilon)\, f'(\phi) + \Delta x'(\phi) + i\,\Delta y'(\phi)$$

Let q be the local total velocity, then $q = \sqrt{u^2 + v^2}$

and we have

$$\frac{q}{V} = \frac{2S(1+\epsilon)}{\pi}\left[\frac{\cosh\psi\cos(\alpha+\beta)\sin\phi - \sinh\psi\sin(\alpha+\beta)\cos\phi + \frac{\Gamma}{4VS}\sinh 2\psi}{(\cosh 2\psi - \cos 2\phi)\sqrt{\left[(1+\epsilon)f'(\phi) + \Delta x'(\phi)\right]^2 + \left[\Delta y'(\phi)\right]^2}}\right] \tag{16}$$

If we satisfy the Kutta condition at the trailing edge we obtain

$$\frac{\Gamma}{2VS} = \frac{\cos\phi_T}{\cosh\psi}\sin(\alpha+\beta) - \frac{\sin\phi_T}{\sinh\psi}\cos(\alpha+\beta) \tag{17}$$

so the velocity distribution becomes

$$\frac{q}{V} = \frac{2S(1+\epsilon)}{\pi}\left[\frac{\cosh\psi\cos(\alpha+\beta)(\sin\phi - \sin\phi_T) - \sinh\psi\sin(\alpha+\beta)(\cos\phi - \cos\phi_T)}{(\cosh 2\psi - \cos 2\phi)\sqrt{\left[(1+\epsilon)f'(\phi) + \Delta x'(\phi)\right]^2 + \left[\Delta y'(\phi)\right]^2}}\right] \tag{18}$$

With this equation, we have the complete solution for the two dimensional flow about airfoils in a cascade. It should be noted, however, that the velocity entering the cascade is not the velocity used in the equation. The entering velocity must be altered as shown in the velocity diagram (Fig. 5) to obtain the velocity used in the equation.

PART III

NUMERICAL PROCEDURE FOR THE CASCADE TRANSFORMATION

The procedure is given in the following steps.

1. Plot the airfoil section on a large sheet of graph paper using an expanded scale in the y-direction for accuracy. Make the plot in such a manner that the leading edge of the airfoil is tangent to the line x=0 and the trailing edge tangent to the line x=1. From this plot, make accurate measurements of the slope $\left(\frac{dy}{dx}\right)$ of the airfoil and plot these against x. It is important that this curve be accurate, therefore, it should be checked by integrating back to see if the airfoil shape results. The gap-chord ratio (S) and the cascade angle (β) are known. Using these, the value of ψ is determined from the equation

$$\frac{1}{2}\cos\beta \log \frac{\sqrt{(\cosh 2\psi + \cos 2\beta)\frac{1}{2}} + \cos\beta}{\sqrt{(\cosh 2\psi + \cos 2\beta)\frac{1}{2}} - \cos\beta} + \sin\beta \tan^{-1} \frac{\sin\beta}{\sqrt{(\cosh 2\psi + \cos 2\beta)\frac{1}{2}}} = \frac{\pi}{2S} \quad *$$

2. With ψ determined evaluate the functions $f(\phi)$ and $f'(\phi)$ where

$$f(\phi) = \frac{1}{2} + \frac{S}{\pi}\left[\frac{1}{2}\cos\beta \log \frac{\cosh\psi + \cos\phi}{\cosh\psi - \cos\phi} + \sin\beta \tan^{-1} \frac{\sin\phi}{\sinh\psi}\right] \quad **$$

and $$f'(\phi) = \frac{S}{\pi} \frac{\sin\beta \sinh\psi \cos\phi - \cos\beta \cosh\psi \sin\phi}{(\sinh\psi)^2 + (\sin\phi)^2}$$

Plot these functions against ϕ . we see that $f(\pi+\phi) = 1 - f(\phi)$ and $f'(\pi+\phi) = -f'(\phi)$, so that only half the range from 0 to 2π needs to be plotted.

---

*This is equation 5 rewritten.

**Equation 6 rewritten using ——?—— $\zeta = e^{i\phi}$

3. Divide the circle into (N) odd divisions so that $\phi_j = j\frac{2\pi}{N}$ with $j = 0, 1, 2, \cdots, N-1$. For the first approximation,

let $X_j = f(\phi_j)$ and $\left(\frac{dx}{d\phi}\right)_j = f'(\phi_j)$

Using this, determine

$$\left(\frac{dy}{d\phi}\right)_j = \left(\frac{dx}{d\phi}\right)_j \left(\frac{dy}{dx}\right)_j$$

where $\left(\frac{dy}{dx}\right)_j$ is obtained from the plot of $\frac{dy}{dx}$ prepared in step 1. From the values of $\left(\frac{dy}{d\phi}\right)_j$ obtain

$$\frac{dy}{d\phi} \simeq \sum_{n=1}^{\frac{N-1}{2}} \left[-nB_n \sin(n\phi) - nA_n \cos(n\phi)\right]$$

by using the table for the value of N selected from Stumpff's, "Tafeln Und Aufgaben Zur Harmonischen Analyse Und Periodogrammrechnung." (10)*

3(a). We see that at the leading and trailing edges of the airfoil $\frac{dy}{dx}$ goes to infinity while $\frac{dx}{d\phi}$ goes to zero, thus giving an indeterminate quantity. If the nose or trailing edges of the airfoil can be approximated by a circle or parabola, the following methods can be used for determining $\frac{dy}{d\phi}$ in the vicinity where these values

---

*For the first approximation, a smaller number of divisions (N) can be used and this increased in the later approximations to obtain the final desired accuracy. In obtaining the results for this paper 11 divisions were used on the first approximation and this increased to 17 for the remaining approximations. These tables are included in appendix A.

become indeterminate. In the case of a circle, the general equation is $(x-a)^2 + (y-b)^2 = c^2$. Taking the first derivative with respect to ϕ , we obtain $(x-a)\frac{dx}{d\phi} + (y-b)\frac{dy}{d\phi} = 0$ and

$$\frac{dy}{d\phi} = -\frac{(x-a)}{(y-b)}\frac{dx}{d\phi}$$

As the nose of the airfoil is approached $y-b$ and $\frac{dx}{d\phi}$ go to zero. Applying L'Hospital's rule, we obtain

$$\frac{dy}{d\phi} = -\frac{\left(\frac{dx}{d\phi}\right)^2 + (x-a)\frac{d^2x}{d\phi^2}}{\frac{dy}{d\phi}}$$

As the nose is approached $\frac{dx}{d\phi}$ and x go to zero and we obtain in the limit

$$\left(\frac{dy}{d\phi}\right)^2_{\phi_L} = a\left(\frac{d^2x}{d\phi^2}\right)_{\phi_L}$$

In the case of a parabola, the general equation is $(ax+by-c)^2 = A(bx-ay+d)$. Following the same procedure as above, we obtain

$$\frac{dy}{d\phi} = \frac{2a\left(a\frac{dx}{d\phi} + b\frac{dy}{d\phi}\right)\frac{dx}{d\phi} + \left[2a(ax+by-c) - Ab\right]\frac{d^2x}{d\phi^2}}{-2b\left[a\frac{dx}{d\phi} + b\frac{dy}{d\phi}\right]}$$

As the nose is approached, $\frac{dx}{d\phi}$ and x go to zero, ϕ approaches ϕ_L, and y approaches y_L . We obtain in the limit

$$\left(\frac{dy}{d\phi}\right)^2_{\phi_L} = -\frac{2a(by_L - c) - Ab}{2b^2}\left(\frac{d^2x}{d\phi^2}\right)_{\phi_L}$$

In the case where a simple parabola is used, $a = 0$ giving

$$\left(\frac{dy}{d\phi}\right)^2 = \frac{A}{2b}\frac{d^2X}{d\phi^2}$$

which holds over the entire range that the equation approximates the nose of the airfoil. In the cases above, however, where $\frac{dy}{d\phi}$ is found only at the nose, there will be a small range in which $\frac{dy}{d\phi}$ is indeterminate. This is the range between the nose and the point where $\frac{dy}{dX}$ becomes small enough to be read from the curve of $\frac{dy}{dx}$ versus x. If we plot $\frac{dy}{d\phi}$ against ϕ, the value of $\left(\frac{dy}{d\phi}\right)_{\phi_L}$ plotted against ϕ_L will enable us to fill in the curve in this region and estimate quite accurately the value of $\frac{dy}{d\phi}$ in the intermediate range. The above discussion has dealt with the nose of the airfoil, but it is obvious that the same procedure can be applied to the trailing edge.

Since

$$X = (1+\epsilon)f(\phi) + \Delta X(\phi) + \delta \quad \text{(equation 9)},$$

then $$\frac{d^2X}{d\phi^2} = (1+\epsilon)f''(\phi) + \Delta X''(\phi)$$

where $$f''(\phi) = \frac{\delta}{\pi}\left[-\frac{\sin\beta\sinh\psi\sin\phi + \cos\beta\cosh\psi\cos\phi}{\sinh^2\psi + \sin^2\phi} - \frac{\sin\beta\sinh\psi\cos\phi - \cos\beta\cosh\psi\sin\phi}{(\sinh^2\psi + \sin^2\phi)^2}(2\sin\phi\cos\phi)\right]$$

and $$\Delta X''(\phi) = \sum_{n=1}^{\frac{N-1}{2}}\left[-A_n n^2\cos(n\phi) - B_n n^2\sin(n\phi)\right]$$

Again it is noted that for the first approximation $\frac{d^2X}{d\phi^2} = f''(\phi)$ is used.

4. The angles corresponding to the leading edge ϕ_L and the trailing edge ϕ_T are first approximated by $f'(\phi) = 0$

Succeeding determinations of the angles are made by the equations $-(1+\epsilon)f'(\phi_T) = \Delta X'(\phi_T)$ and $-(1+\epsilon)f'(\phi_L) = \Delta X'(\phi_L)$ Initially, let $\epsilon = 0$ and determine ϕ_T and ϕ_L by plotting $-f'(\phi)$ and $\Delta X'(\phi)$ against ϕ and reading the intersection. Using these values, determine ϵ from the equation

$$\epsilon = \frac{1 - f(\phi_T) + f(\phi_L) - \Delta X(\phi_T) + \Delta X(\phi_L)}{f(\phi_T) - f(\phi_L)}$$

With this value of ϵ, replot $-(1+\epsilon)f(\phi)$ and read the new intersections. Repeat this procedure until there is no appreciable change in the values of ϕ_T and ϕ_L. When this is done, determine the constant δ from the equation.

$$\delta = 1 - (1+\epsilon)f(\phi_T) - \Delta X(\phi_T)$$

5. The new expression for x is now $X = (1+\epsilon)f(\phi) + \Delta X(\phi) + \delta$ We use this expression to determine

$$X_j = (1+\epsilon)f(\phi_j) + \Delta X(\phi_j) + \delta$$

$$\left(\frac{dX}{d\phi}\right)_j = (1+\epsilon)f'(\phi_j) + \Delta X'(\phi_j)$$

from $j = 0, 1, 2, \cdots N-1$. Using these new values, determine $\left(\frac{dy}{d\phi}\right)_j$ as described in step 3 and then determine the new values for A_n and B_n from $\left(\frac{dy}{d\phi}\right)_j$.

6. Repeat step 4 using the value of ϵ previously determined in the first application of step 4 in obtaining ϕ_T and ϕ_L. After determining the new ϕ_T and ϕ_L, repeat step 5 and obtain new values for $\left(\frac{dy}{d\phi}\right)_j$. Continue this cycle of steps 4 and 5, until the new

values of $\left(\frac{dy}{d\phi}\right)_j$ obtained show very little change over the previous values.

7. The Kutta condition gives the circulation around any airfoil in the cascade as

$$\frac{\Gamma}{2VS} = \frac{\cos\phi_T}{\cosh\psi}\sin(\alpha+\beta) - \frac{\sin\phi_T}{\sinh\psi}\cos(\alpha+\beta)$$

The velocity diagram for the cascade is shown in Fig. 5. We can solve for γ_e from Fig. 5 in terms of γ_i and obtain

$$\cot\gamma_e = \frac{\cosh\psi - \cos\phi_T}{\cosh\psi + \cos\phi_T}\cot\gamma_i + \frac{2\coth\psi\sin\phi_T}{\cosh\psi+\cos\phi_T} \qquad (19)$$

The angle of attack α for any incidence angle γ_i can be found from the relationship

$$\tan(\alpha+\beta) = \frac{\sinh\psi\cot\gamma_i + \sin\phi_T}{\tanh\psi(\cosh\psi+\cos\phi_T)} \qquad (20)$$

and for any exit angle γ_e the relationship is

$$\tan(\alpha+\beta) = \frac{\sinh\psi\cot\gamma_e - \sin\phi_T}{\tanh\psi(\cosh\psi-\cos\phi_T)} \qquad (21)$$

The lift coefficient is given by the equation $C_L = \frac{2\Gamma}{bV}$ based on the mean velocity and the chord (in this case equal to unity). Putting Γ into the equation, we obtain

$$C_L = 4S\left[\frac{\cos\phi_T}{\cosh\psi}\sin(\alpha+\beta) - \frac{\sin\phi_T}{\sinh\psi}\cos(\alpha+\beta)\right] \qquad (22)$$

8. Having satisfied the Kutta condition, we can now determine the velocity distribution about the airfoil as a function of ϕ by the following relationship,

$$\frac{q}{V} = \frac{s(1+\epsilon)}{\pi} \frac{\cosh\psi \cos(\alpha+\beta)(\sin\phi - \sin\phi_T) - \sinh\psi \sin(\alpha+\beta)(\cos\phi - \cos\phi_T)}{\left[\sinh^2\psi + \sin^2\phi\right]\sqrt{\left[(1+\epsilon)f'(\phi) + \Delta x'(\phi)\right]^2 + \left[\Delta y'(\phi)\right]^2}} *$$

Probably the easiest way to plot the complete distribution of velocity about the airfoil is to plot X , $\frac{dx}{d\phi}$, and $\frac{dy}{d\phi}$ against ϕ . This is done from the equations

$$X = (1+\epsilon) f(\phi) + \Delta X(\phi) + \delta$$

$$\frac{dx}{d\phi} = (1+\epsilon) f'(\phi) + \Delta X'(\phi)$$

$$\frac{dy}{d\phi} = \Delta y'(\phi)$$

The plot of x enables us to find the position in the Z - plane corresponding to any chosen value of ϕ , while the plot of the other two factors enables us to determine the radical $\sqrt{\left[(1+\epsilon)f'(\phi) + \Delta x'(\phi)\right]^2 + \left[\Delta y'(\phi)\right]^2}$ for any ϕ . Thus knowing ϕ and the above values, we can determine the velocity distribution about the airfoil for any angle of attack.

---

*This is equation 18 rewritten.

PART IV

CALCULATIONS AND RESULTS

Three cascade sections were calculated for the pump. They are the hub, mid-section of the blade, and tip of the blade. Since the hub blade section is thickest and the cascade at the hub has the lowest gap-chord ratio, the hub solution offers the most interesting results. For this reason, the complete calculations are given for the hub section, while only the results are presented for the other two sections. Enough of the results for these sections are listed, however, to give some idea of the rapidity of the convergence with successive approximations.

(a)

Hub Airfoil Data

The hub section is made of NACA airfoil 4412. The dimensions were altered from those of NACA report 460 (11) to bring the nose tangent to the line x=0. The following table gives the dimensions used in this paper for the airfoil.

airfoil station $X \times 100$	upper surface $y \times 100$	lower surface $y \times 100$
0	0	0
1.25	2.13	-1.74
2.5	3.08	-2.26
5.0	4.43	-2.79
7.5	5.47	-3.03
10.0	6.31	-3.14
15.0	7.62	-3.15
20.0	8.55	-2.99
25.0	9.17	-2.74
30.0	9.54	-2.48
40.0	9.61	-1.99
50.0	9.03	-1.56
60.0	8.01	-1.13
70.0	6.60	-0.74
80.0	4.83	-0.45
90.0	2.68	-0.25
95.0	1.45	-0.18
100.0	0.13	-0.13

The leading edge of the airfoil is given by the following equation

$$(x-.0158)^2 + y^2 = (.0158)^2$$

The trailing edge is approximated by

$$(x-.0013)^2 + y^2 = (.0013)^2$$

Using this data, we determine the slope curves for the airfoil given in Fig. 6.

Pump Data

Section radius = 1.80''

Chord length = 3.25''

Cascade angle = $\beta = 56.40^\circ$

The pump is an axial flow type with three blades.

1.

Calculations

From the equation

$$\frac{\pi}{2S} = \frac{1}{2}\cos\beta \log \frac{\sqrt{\frac{1}{2}(\cosh 2\psi + \cos 2\beta)} + \cos\beta}{\sqrt{\frac{1}{2}(\cosh 2\psi + \cos 2\beta)} - \cos\beta} + \sin\beta \tan^{-1} \frac{\sin\beta}{\sqrt{\frac{1}{2}(\cosh 2\psi + \cos 2\beta)}}$$

and letting $P = \sqrt{\frac{1}{2}(\cosh 2\psi + \cos 2\beta}$, we can solve for ψ

We have $\frac{S}{\pi} = \frac{2\pi R}{\pi 3C} = 0.369$, $\beta = 56.4^\circ$, $\sin\beta = 0.833$, and $\cos\beta = 0.553$

Then we obtain

$$0.553 \log \frac{P + 0.553}{P - 0.553} + 1.666 \tan^{-1} \frac{0.833}{P} = 2.71$$

By trial and error, we obtain

$$P = 0.684 \text{ and } \psi = 0.390$$

The equation for $f(\phi)$ is

$$f(\phi) = \frac{1}{2} + \frac{S}{\pi}\left(\frac{1}{2}\cos\beta \log \frac{\cosh\psi + \cos\phi}{\cosh\psi - \cos\phi} + \sin\beta \tan^{-1} \frac{\sin\phi}{\sinh\psi}\right)$$

Thus we have,

$$f(\phi) = \frac{1}{2} + 0.102 \log \frac{1.077 + \cos\phi}{1.077 - \cos\phi} + 0.307 \tan^{-1} \frac{\sin\phi}{0.400}$$

The equation for $f'(\phi)$ is

$$f'(\phi) = \frac{S}{\pi} \frac{\sin\beta \sinh\psi \cos\phi - \cos\beta \cosh\psi \sin\phi}{\sinh^2\psi + \sin^2\phi}$$

Thus we have,

$$f'(\phi) = \frac{0.123 \cos\phi - 0.220 \sin\phi}{0.160 + \sin^2\phi}$$

These equations are plotted and the curves are shown in Fig. 7 and 8.

Dividing the circle into 11 sectors, we obtain the following table

j	ϕ_j	$X_j = f(\phi_j)$	$\left(\frac{dx}{d\phi}\right)_j = f'(\phi_j)$	$\left(\frac{dy}{dx}\right)_{X_j}$	$\left(\frac{dy}{d\phi}\right)_j$
0	0	0.836	0.769	0.020	0.0153
1	32.73	0.999	−0.032	−0.156	0.0050
2	64.45	0.940	−0.149	−0.251	0.0374
3	98.19	0.870	−0.208	−0.225	0.0469
4	130.91	0.788	−0.334	−0.194	0.0649
5	163.64	0.395	−0.750	−0.025	0.0188
6	196.36	0.020	−0.230	0.710	−0.1631
7	239.09	0.022	0.120	−0.330	−0.0396
8	261.82	0.109	0.176	−0.017	−0.0030
9	294.55	0.228	0.252	0.049	0.0123
10	237.27	0.428	0.495	0.043	0.0213

Using table 1 in appendix A, we obtain the following equation

$$\Delta y'(\phi) = \frac{dy}{d\phi} = \sum_{n=1}^{5}\left[-n B_n \sin(n\phi) - n A_n \cos(n\phi)\right]$$

where

$A_1 = -0.0315$ $\qquad$ $B_1 = -0.0268$

$2A_2 = +0.0315$ $\qquad$ $2B_2 = +0.0454$

$3A_3 = -0.0178$ $\qquad$ $3B_3 = -0.0254$

$4A_4 = +0.0102$ $\qquad$ $4B_4 = +0.0175$

$5A_5 = -0.0062$ $\qquad$ $5B_5 = -0.0239$

From this, we obtain

$$\Delta X(\phi) = \sum_{n=1}^{5}\left[A_n \cos(n\phi) + B_n \sin(n\phi)\right]$$

and differentiating this, we get

$$\Delta X'(\phi) = \sum_{n=1}^{5} \left[- n A_n \sin(n\phi) + n B_n \cos(n\phi) \right]$$

From the plot of $f'(\phi)$, we see that $\phi_T \approx 29.5^\circ$ and $\phi_L \approx \pi + 29.5^\circ$ as a first approximation. Plotting $-\Delta X'(\phi)$ on $f'(\phi)$ in the vicinity of these two values, we obtain $\phi_T = 30.4^\circ$ and $\phi_L = \pi + 42.6^\circ$. Since the first approximations are all crude, there is no need to resolve for ϕ_T and ϕ_L after obtaining ϵ for this first approximation. Thus we find

$$f(\phi_T) = 1.000,\ f(\phi_L) = 0.010,\ \Delta X(\phi_T) = -0.020,\ \Delta X(\phi_L) = 0.066$$

Therefore
$$\epsilon = \frac{1 - f(\phi_T) + f(\phi_L) - \Delta X(\phi_T) + \Delta X(\phi_L)}{f(\phi_T) - f(\phi_L)} = 0.097$$

$$\delta = 1 - (1+\epsilon) f(\phi_T) - \Delta X(\phi_T) = -0.077$$

$$X = (1+\epsilon) f(\phi) + \sum_{n=1}^{5} \left[A_n \cos(n\phi) + B_n \sin(n\phi) \right] + \delta$$

$$\frac{dX}{d\phi} = (1+\epsilon) f'(\phi) + \sum_{n=1}^{5} \left[- n A_n \sin(n\phi) + n B_n \cos(n\phi) \right]$$

$$x = (1.097)\, f(\phi) + \Delta X(\phi) - 0.077$$

$$\frac{dx}{d\phi} = (1.097)\, f'(\phi) + \Delta X'(\phi)$$

For the second approximation, we divide the circle into 17 sectors. Since we will use this same number of divisions for the rest of the approximations, the following table is given using the ϕ_j's obtained from table 2 of appendix A.

j	ϕ_j	$f(\phi_j)$	$f'(\phi_j)$
0	0	0.836	0.769
1	21.18	0.996	0.128
2	42.35	0.989	-0.093
3	63.63	0.942	-0.149
4	84.71	0.881	-0.181
5	105.88	0.809	-0.227
6	127.06	0.709	-0.310
7	148.29	0.545	-0.510
8	169.41	0.316	-0.842
9	190.59	0.055	-0.410
10	211.76	0.000	0.025
11	232.94	0.030	0.130
12	254.12	0.088	0.164
13	275.39	0.153	0.201
14	296.57	0.238	0.260
15	317.75	0.357	0.388
16	338.92	0.545	0.665

For the second approximation we obtain the following table.

j	$\Delta x(\phi_j)$	$X_j = (1+\epsilon) f(\phi_j) + \Delta x(\phi_j) + \delta$	$\Delta x'(\phi_j)$	$\left(\frac{dx}{d\phi}\right)_j = (1+\epsilon) f'(\phi_j) + \Delta x'(\phi_j)$	$\left(\frac{dy}{dx}\right)_{x_j}$	$\left(\frac{dy}{d\phi}\right)_j$
0	-0.020	0.821	-0.013	0.831	0.023	0.0191
1	-0.022	0.994	0.007	0.148	0.009	0.0013
2	-0.018	0.989	0.002	-0.100	-0.270	0.0270
3	-0.025	0.931	-0.032	-0.195	-0.248	0.0484
4	-0.035	0.854	-0.017	-0.215	-0.219	0.0471
5	-0.036	0.774	0.008	-0.241	-0.188	0.0454
6	-0.032	0.669	0.013	-0.327	-0.147	0.0481
7	-0.018	0.503	0.065	-0.495	-0.082	0.0405
8	0.029	0.299	0.156	-0.769	0.052	-0.0400
9	0.077	0.061	0.079	-0.371	0.414	-0.1538
10	0.079	0.002	-0.081	-0.053	--	-0.0900*
11	0.046	0.002	-0.087	0.055	--	-0.0400*
12	0.022	0.042	-0.046	0.134	-0.172	-0.0231
13	0.005	0.096	-0.052	0.168	-0.031	-0.0052
14	-0.014	0.170	-0.042	0.243	0.030	0.0073
15	-0.021	0.294	0.004	0.436	0.055	0.0237
16	-0.018	0.503	0.004	0.734	0.043	0.0315

*See page 30 for details of how these values were determined.

We see that numbers 10 and 11 of the second approximation are too close to the leading edge to allow $\frac{dy}{dx}$ to be read from the curve. The equation for the curve at the leading edge is the following circle.

$$(x - 0.0158)^2 + y^2 = (0.0158)^2$$

From this, we obtain

$$0.0158\left(\frac{d^2x}{d\phi^2}\right)_{\phi_L} = \left(\frac{dy}{d\phi}\right)^2_{\phi_L}$$

where $\frac{d^2x}{d\phi^2} = (1+\epsilon) f''(\phi) + \Delta x''(\phi)$

and

$$f''(\phi) = \frac{-0.123 \sin\phi - 0.220 \cos\phi}{0.160 + \sin^2\phi} - \frac{0.123 \cos\phi - 0.220 \sin\phi}{(0.160 + \sin^2\phi)^2} (2 \sin\phi\cos\phi$$

Since $\phi = \pi + 42.6^\circ$, we obtain $f''(\phi_L) = 0.244$ and $\Delta x''(\phi_L) = -0.089$ and thus get $\left(\frac{d^2x}{d\phi^2}\right)_{\phi_L} = 0.179$

Therefore, we have

$$\left(\frac{dy}{d\phi}\right)_{\phi_L} = -0.0531$$

By plotting $\frac{dy}{d\phi}$ against ϕ and reading the values for 10 and 11 from the plot, we obtain values for those points where $\frac{dy}{dx}$ cannot be directly determined. The value at ϕ_L is between the two points and allows us to fill in the range for the missing points quite readily.

Using table 2 in appendix A, we obtain the following coefficients

$A_1 = -0.0397$	$B_1 = -0.0360$
$2A_2 = +0.0295$	$2B_2 = +0.0298$
$3A_3 = -0.0142$	$3B_3 = -0.0110$
$4A_4 = +0.0134$	$4B_4 = +0.0190$
$5A_5 = -0.0091$	$5B_5 = -0.0060$
$6A_6 = +0.0033$	$6B_6 = +0.0084$
$7A_7 = -0.0027$	$7B_7 = -0.0050$
$8A_8 = -0.0004$	$8B_8 = +0.0038$

where $$\Delta X(\phi) = \sum_{n=1}^{8} \left[A_n \cos(n\phi) + B_n \sin(n\phi)\right]$$

$$\Delta X'(\phi) = \sum_{n=1}^{8} \left[-n A_n \sin(n\phi) + n B_n \cos(n\phi)\right]$$

Plotting $-\Delta X'(\phi)$ on $(1+\epsilon) f'(\phi)$, where ϵ here is the previously determined ϵ, we obtain from the intersections $\phi_T = 27.4^\circ$ and $\phi_L = \pi + 35.8^\circ$. Then, $f(\phi_T) = 1.000$, $f(\phi_L) = 0.003$, $\Delta X(\phi_T) = -0.032$, $\Delta X(\phi_L) = 0.069$, $\epsilon = 0.104$, and $\delta = -0.104 + 0.032 = -0.072$ The ϵ in this case being close enough to the original ϵ, the procedure need not be repeated.

Thus, we have

$$x = (1.104) f(\phi) + \Delta X(\phi) - 0.072$$

$$\frac{dx}{d\phi} = (1.104) f'(\phi) + \Delta X'(\phi)$$

For the third approximation, we obtain the following table.

j	$\Delta X(\phi_j)$	X_j	$\Delta X'(\phi_j)$	$\left(\frac{dx}{d\phi}\right)_j$	$\left(\frac{dy}{dx}\right)_{x_j}$	$\left(\frac{dy}{d\phi}\right)_j$
0	-0.027	0.824	0.003	0.852	0.021	0.0179
1	-0.029	0.998	-0.019	0.122	0.009	0.0011
2	-0.040	0.980	-0.030	-0.133	-0.266	0.0354
3	-0.047	0.921	-0.008	-0.173	-0.245	0.0424
4	-0.046	0.855	0.015	-0.185	-0.220	0.0407
5	-0.039	0.783	0.020	-0.231	-0.192	0.0444
6	-0.028	0.683	0.044	-0.298	-0.153	0.0457
7	-0.004	0.526	0.089	-0.474	-0.092	0.0436
8	0.041	0.318	0.145	-0.785	0.035	-0.0274
9	0.082	0.071	0.047	-0.406	0.382	-0.1550
10	0.073	0.001	-0.063	-0.035	--	-0.1000*
11	0.053	0.015	-0.046	0.097	-0.425	-0.0412
12	0.035	0.060	-0.051	0.130	-0.105	-0.0137
13	0.017	0.114	-0.047	0.175	-0.013	-0.0023
14	-0.003	0.188	-0.050	0.237	0.038	0.0090
15	-0.016	0.306	-0.033	0.395	0.054	0.0213
16	-0.026	0.504	-0.016	0.719	0.045	0.0324

*See page 33 for details of how this value was determined.

For $\phi = \pi + 35.8^{\circ}$, we obtain

$$f''(\phi_L) = 0.390 \text{ and } \Delta x''(\phi_L) = 0.020$$

Since

$$\left(\frac{dy}{d\phi}\right)^2_{\phi_L} = 0.0158 \left(\frac{d^2x}{d\phi^2}\right)_{\phi_L} \quad \text{and} \quad \left(\frac{d^2x}{d\phi^2}\right)_{\phi_L} = 0.451$$

we obtain

$$\left(\frac{dy}{d\phi}\right)_{\phi_L} = -0.0845$$

By plotting $\frac{dy}{d\phi}$ against ϕ and reading the value for number 10 from the plot, we obtain the value of $\frac{dy}{d\phi}$ at this point for which $\frac{dy}{dx}$ cannot be read.

At this time, a check can be made which will show if the $\frac{dy}{d\phi}$ is approaching close to the final solution. We know there can be no constant term for $\Delta y'(\phi)$, therefore, $\sum_{j=0}^{\infty} \left(\frac{dy}{d\phi}\right)_j = 0$. For the second approximation, we obtain $\sum_{j=0}^{16} \left(\frac{dy}{d\phi}\right)_j = -0.0127$ and for the third approximation $\sum_{j=0}^{16} \left(\frac{dy}{d\phi}\right)_j = -0.0057$ which indicates the third approximation is fairly close to the answer.

Using table 2 from appendix A, we obtain the coefficients for the third approximation.

$A_1 = -0.0381$ $\quad$ $B_1 = -0.0347$

$2A_2 = 0.0286$ $\quad$ $2B_2 = 0.0308$

$3A_3 = -0.0134$ $\quad$ $3B_3 = -0.0162$

$4A_4 = 0.0121$ $\quad$ $4B_4 = 0.0211$

$5A_5 = -0.0053$ $\quad$ $5B_5 = -0.0066$

$6A_6 = 0.0026$ $\quad$ $6B_6 = 0.0094$

$7A_7 = -0.0033$ $\quad$ $7B_7 = -0.0039$

$8A_8 = -0.0005$ $\quad$ $8B_8 = 0.0051$

Again plotting $-\Delta x'(\phi)$ on $(1+\epsilon) f'(\phi)$, we obtain $\phi_T = 27.4^\circ$ and $\phi_L = \pi + 36.1^\circ$ for the final approximation using the new ϵ. Then $f(\phi_T) = 1.000$, $f(\phi_L) = 0.003$, $\Delta x(\phi_T) = -0.031$, $\Delta x(\phi_L) = 0.071$, and $\epsilon = 0.105$, and therefore,

$\delta = -0.105 + 0.031 = -0.074$

Thus, we have

$$x = (1.105) f(\phi) + \Delta x(\phi) - 0.074$$

$$\frac{dx}{d\phi} = (1.105) f'(\phi) + \Delta x'(\phi)$$

For the fourth approximation, we obtain the following table.

j	$\Delta x(\phi_j)$	x_j	$\Delta x'(\phi_j)$	$\left(\frac{dx}{d\phi}\right)_j$	$\left(\frac{dy}{dx}\right)_{x_j}$	$\left(\frac{dy}{d\phi}\right)_j$
0	−0.026	0.824	0.006	0.856	0.021	0.0180
1	−0.028	0.998	−0.021	0.120	0.009	0.0011
2	−0.038	0.980	−0.026	−0.129	−0.266	0.0343
3	−0.044	0.923	−0.002	−0.167	−0.245	0.0410
4	−0.043	0.857	0.011	−0.189	−0.221	0.0418
5	−0.038	0.782	0.019	−0.232	−0.191	0.0443
6	−0.027	0.682	0.041	−0.301	−0.152	0.0458
7	−0.006	0.522	0.078	−0.485	−0.090	0.0436
8	0.037	0.312	0.137	−0.793	0.040	−0.0317
9	0.080	0.067	0.067	−0.386	0.395	−0.1521
10	0.076	0.002	−0.059	−0.031	--	−0.0980*
11	0.053	0.013	−0.057	0.086	−0.475	−0.0409
12	0.035	0.058	−0.056	0.125	−0.114	−0.0142
13	0.015	0.110	−0.049	0.173	−0.018	−0.0031
14	−0.001	0.188	−0.047	0.240	0.038	0.0091
15	−0.015	0.305	−0.030	0.398	0.055	0.0219
16	−0.024	0.504	−0.020	0.715	0.045	0.0322

*See page 36 for details of how this value was determined.

For $\phi_L = \pi + 36.1^\circ$, we obtain

$$f''(\phi_L) = 0.390 \text{ and } \Delta X''(\phi_L) = -0.025$$

Therefore $$\left(\frac{d^2x}{d\phi^2}\right)_{\phi_L} = 0.406$$

and $$\left(\frac{dy}{d\phi}\right)_{\phi_L} = 0.0800$$

Again by plotting $\frac{dy}{d\phi}$ against ϕ, we are able to obtain the indeterminate point 10. By plotting $(1+\epsilon) f'(\phi)$ on $-\Delta X'(\phi)$, we obtain $\phi_L = \pi + 36.1^\circ$ and $\phi_T = 27.4^\circ$

Then $f(\phi_T) = 1.000$, $f(\phi_L) = 0.003$, $\Delta X(\phi_T) = -0.032$, $\Delta X(\phi_L) = 0.071$ and therefore, $\epsilon = 0.106$ and $\delta = -0.075$

Since there was not much change in $\frac{dy}{d\phi}$ for the last two approximations, we use this last approximation as the final answer. Thus we have,

$$x = (1.106) f(\phi) + \Delta X(\phi) - 0.075$$

$$y = \Delta y(\phi)$$

For the coefficients, we have

$A_1 = -0.0392$	$B_1 = -0.0345$
$2A_2 = 0.0285$	$2B_2 = 0.0299$
$3A_3 = -0.0138$	$3B_3 = -0.0152$
$4A_4 = 0.0125$	$4B_4 = 0.0201$
$5A_5 = -0.0055$	$5B_5 = -0.0064$
$6A_6 = 0.0030$	$6B_6 = 0.0098$
$7A_7 = -0.0035$	$7B_7 = -0.0031$
$8A_8 = -0.0007$	$8B_8 = 0.0046$

The equation for the lift coefficient is

$$C_L = 4S\left[\frac{\cos\phi_T}{\cosh\psi}\sin(\alpha+\beta) - \frac{\sin\phi_T}{\sinh\psi}\cos(\alpha+\beta)\right]$$

Since $S = 1.16$, $\cos\phi_T = 0.888$, $\sin\phi_T = 0.460$, $\cosh\psi = 1.077$ $\sinh\psi = 0.400$, $\sin\beta = 0.833$, and $\cos\beta = 0.553$, we have

$$C_L = 3.82\sin(\alpha+\beta) - 5.33\cos(\alpha+\beta)$$

By rewriting, we obtain

$$C_L = 6.59\sin(\alpha + 2.00^\circ)$$

For convenience of showing the convergence of the successive approximations, a table of $\frac{dy}{d\phi}$ for the various approximations is given.

$\left(\frac{dy}{d\phi}\right)_j$

j	2nd Approx.	3rd Approx.	4th Approx.
0	0.0191	0.0179	0.0180
1	0.0015	0.0011	0.0011
2	0.0270	0.0354	0.0343
3	0.0484	0.0424	0.0410
4	0.0471	0.0407	0.0418
5	0.0454	0.0444	0.0443
6	0.0481	0.0457	0.0458
7	0.0405	0.0436	0.0436
8	− 0.0400	− 0.0274	− 0.0317
9	− 0.1538	− 0.1550	− 0.1521
10	− 0.0900	− 0.1000	− 0.0980
11	− 0.0400	− 0.0412	− 0.0409
12	− 0.0231	− 0.0137	− 0.0142
13	− 0.0052	− 0.0023	− 0.0031
14	0.0073	0.0090	0.0091
15	0.0237	0.0213	0.0219
16	0.0315	0.0324	0.0322

(b)

Mid-Section Airfoil Data

The mid-section is made of NACA airfoil 4409.

Pump Data

Section radius = 2.90''

Chord length = 2.91''

Cascade angle = 71.35°

From the above data, we obtain $\frac{s}{\pi} = 0.664$ and $\Psi = 0.950$

For this section, four approximations were used as before. $\left(\frac{dy}{d\phi}\right)_j$ will be listed for the approximations to show the speed of convergence.

Using the final approximation, we obtain for the solution

$$\phi_T = 60.7^\circ \qquad \phi_L = \pi + 71.1^\circ$$

$$\epsilon = 0.081 \qquad \delta = -0.053$$

$$x = (1.081) f(\phi) + \Delta x(\phi) - 0.053$$

$$y = \Delta y(\phi)$$

For the coefficients, we have

$A_1 = -0.0135$	$B_1 = -0.0374$
$2A_2 = 0.0054$	$2B_2 = 0.0427$
$3A_3 = -0.0001$	$3B_3 = -0.0058$
$4A_4 = 0.0007$	$4B_4 = 0.0055$
$5A_5 = -0.0001$	$5B_5 = -0.0022$
$6A_6 = 0.0004$	$6B_6 = 0.0013$
$7A_7 = -0.0004$	$7B_7 = -0.0014$
$8A_8 = 0.0004$	$8B_8 = 0.0014$

The equation of the lift coefficient is

$$C_L = 7.18 \sin(\alpha + 3.84^\circ)$$

Table of $\left(\frac{dy}{d\phi}\right)_j$ For Mid-Section

j	2nd Approx.	3rd Approx.	4th Approx.
0	0.0075	0.0075	0.0075
1	−0.0047	−0.0051	−0.0047
2	−0.0044	−0.0042	−0.0042
3	0.0145	0.0126	0.0120
4	0.0350	0.0328	0.0331
5	0.0521	0.0521	0.0522
6	0.0615	0.0625	0.0620
7	0.0549	0.0539	0.0540
8	0.0158	0.0148	0.0158
9	−0.0536	−0.0538	−0.0535
10	−0.0802	−0.0786	−0.0784
11	−0.0800	−0.0750	−0.0750
12	−0.0545	−0.0490	−0.0490
13	−0.0201	−0.0210	−0.0208
14	0.0059	0.0062	0.0075
15	0.0243	0.0245	0.0248
16	0.0232	0.0233	0.0231

(c)

Tip-Section Airfoil Data

The tip-section is made of NACA airfoil 4406.

Pump Data

Section radius = 4.00''

Chord length = 2.88''

Cascade angle = 78.12°

From the above data, we obtain $\frac{s}{\pi} = 0.926$ and $\psi = 1.284$

For this section, four approximations were used. $\left(\frac{dy}{d\phi}\right)_j$ will again be listed to show convergence.

Again, using the final approximation, we obtain for the final solution

$$\phi_T = 71.9^\circ \qquad \phi_L = \pi + 81.7^\circ$$

$$\epsilon = 0.048 \qquad \delta = -0.032$$

$$x = (1.048) f(\phi) + \Delta x(\phi) - 0.032$$

$$y = \Delta y(\phi)$$

For the coefficients, we have

$A_1 = -0.0035$	$B_1 = -0.0266$
$2A_2 = 0.0009$	$2B_2 = 0.0399$
$3A_3 = 0.0041$	$3B_3 = -0.0019$
$4A_4 = 0.0016$	$4B_4 = 0.0007$
$5A_5 = 0.0016$	$5B_5 = -0.0017$
$6A_6 = -0.0001$	$6B_6 = -0.0002$
$7A_7 = -0.0001$	$7B_7 = -0.0004$
$8A_8 = -0.0013$	$8B_8 = -0.0003$

The equation of the lift coefficient is

$$C_L = 6.89 \sin(\alpha + 3.84^\circ)$$

Table of $\left(\frac{dy}{d\phi}\right)_j$ For Tip-Section

j	2nd Approx.	3rd Approx.	4th Approx.
0	−0.0035	−0.0035	−0.0035
1	−0.0151	−0.0147	−0.0147
2	−0.0137	−0.0132	−0.0134
3	−0.0010	−0.0039	−0.0040
4	0.0193	0.0195	0.0196
5	0.0417	0.0424	0.0425
6	0.0554	0.0540	0.0543
7	0.0482	0.0475	0.0480
8	0.0209	0.0211	0.0210
9	−0.0227	−0.0240	−0.0231
10	−0.0550	−0.0575	−0.0575
11	−0.0636	−0.0616	−0.0626
12	−0.0510	−0.0485	−0.0485
13	−0.0180	−0.0180	−0.0180
14	0.0127	0.0127	0.0128
15	0.0288	0.0308	0.0312
16	0.0141	0.0142	0.0142

PART V

DISCUSSION OF THE CALCULATIONS

An examination of the $\frac{dy}{d\phi}$ tables for the successive approximations shows the maximum variation between the third and fourth approximations to be 0.004 for the hub, 0.001 for the mid-section, and 0.001 for the tip-section. The tables are given to four decimal places in order to show the convergence more clearly, but for the practical case three decimal places are sufficient. Thus, we see that for all practical purposes three approximations were sufficient for the hub cascade. Further examination of the data shows that the tip-section converged more rapidly then the other two sections. This was as expected, first because the gap-chord ratio was the largest, placing the singularities in the ζ -plane farther away from the circle, and secondly because the airfoil was thinner, thus having smaller perturbations. The second approximation for the tip section appears to be accurate enough for all practical purposes.

It should be kept in mind that all the airfoil sections used were of the NACA4400 series, and therefore, all had the same camber. The effect of camber variation on the rapidity of the convergence acts in the same manner as thickness, that is, increasing camber tends to cut down the rapidness of convergence. Since a constant camber was used for the three sections, none of this is shown by the

data; but it is expected that the camber effect will be less than that of thickness.

In Wislicenus' book (12), a plot of lattice effect coefficient (K) is made against the gap-chord ratio for various vane angles. These curves are for flat plates, and K is defined as the value by which the slope of the lift curve for an individual flat plate must be multiplied to obtain that for a plate in a cascade. Reading K for the lattice conditions for the pump, we obtain K = 1.09, 1.17, and 1.08 for the hub, mid-section, and tip, respectively. The slope of the lift curve for a single flat plate is $\frac{dC_L}{d\alpha} = 2\pi$. Multiplying by K gives $\frac{dC_L}{d\alpha} = 6.91$, 7.35, and 6.79 as the slope for a lattice of flat plates. Comparing these values with the actual ones, $\frac{dC_L}{d\alpha} = 6.59$, 7.18, and 6.89, we see the same trend exists, and these values are close to those obtained from the above curve. This shows that the thickness and camber involved do not have much effect on the slope of the lift curves .

In the outer sections, the gap-chord ratio is quite large, therefore, it would be expected that the behavior for the airfoil in the cascade would be similar to a single airfoil, particularly near the angle of zero lift. We see that the zero lift angle is the same (-3.84°) for these two sections, and this value is also very similar to the zero lift angle for the single airfoil as shown in the

NACA TR #460 (11). For the hub-section, however, the value of the zero lift angle (-2.00°) does not compare favorably with the value for the single airfoil, which is approximately equal to -4°. This shows that the three variables, the cascade angle, gap-chord ratio, and airfoil thickness, have combined in such a manner as to cause this change.

Some idea of the effect of the cascade angle on both $\frac{dC_L}{d\alpha}$ and the zero lift angle can be determined by comparison with the results of Katzoff, Finn, and Laurence (1). They worked out the results for a cascade composed of NACA 4412 airfoils, with cascade angle equal to zero, and a gap-chord ratio of 1.032. This compares very closely with the hub cascade for the pump of NACA 4412 airfoils, a gap-chord ratio of 1.16, and cascade angle equal to 56.4°. The results of the cascade for the cascade angle equal zero give the angle of zero lift as -5.94° and the slope of the lift curve as 5.70. Comparing with the cascade for the pump, we have the zero lift angle equal -2.00° and the slope of the lift curve equal 6.59. Since the only variable is essentially the cascade angle, we see that as this angle goes to zero it reduces the slope of the lift curve and increases the zero lift angle. Since the angle of zero lift for the single airfoil is about -4°, we see that at some angle in between the above angles, the effect of the gap-chord ratio is balanced by the cascade angle to give

the same angle of zero lift as the single airfoil. The effect on the slope of the lift curve could have been predicted from the K curves mentioned on page 44. From these curves we obtain the slope of the lift curve equal 4.08 for a cascade of flat plate airfoils with zero cascade angle, which checks very closely to that of the NACA 4412 airfoils. Since these curves predict that the slope will continuously decrease as the cascade angle goes to zero, and the slope as calculated for the single airfoil is equal to 6.8, the point where the same zero lift angle is obtained for the cascade and single airfoil will not give equal slopes of the lift curves.

For the three cascades computed in this paper, the curves of maximum velocity on the upper surface versus angle of attack were obtained, and are shown in Fig. 9. The values of the maximum velocity were obtained by plotting the velocity against the parameter ϕ of the ζ -plane, and determining the maximum velocity from the curve. Reading the value of ϕ opposite the maximum velocity, the point on the airfoil where this maximum occurs can then be obtained by substituting this value of ϕ in the final expression obtained for x.

The tip and mid-section airfoils being quite far apart show maximum velocity curves that are similar to those which would beexpected for single airfoils of these thick-

nesses. The thickest of the two airfoils has the highest maximum velocity at low angles of attack, while the thinnest airfoil shows the most rapid rise of maximum velocity with angle of attack. For the hub section, however, we see that it has lower velocities than the mid-section at low angles of attack. Since the hub-section is thickest, this is the opposite of what is expected. This condition is due to the change of circulation around the hub-section because of the cascade effects. Comparing the equations of the lift coefficient (C_L) for the two sections, we see that the angle of zero lift for the hub-section was moved 1.84° in the direction of positive angle of attack. Thus, we see that the circulation has been quite radically changed for the same angle of attack. If we move over on the curve of maximum velocity for the hub-section 1.84°, we see that this velocity will exceed that of the mid-section at the point 1.84° away. This is what we would expect, because this condition is for approximately the same circulation around each airfoil.

The complete velocity distribution curves are given for the hub cascade with both zero and a five degree angle of attack in figures 10 and 11. From figure 10, we see that the maximum velocity on the upper surface of the airfoil is exceeded by the maximum velocity on the lower surface. This is because the zero angle of attack is so near the

zero lift angle. For the five degree angle of attack, this condition disappears, as shown in figure 11, because the angle of attack is now sufficiently larger than the zero lift angle.

The curves of maximum velocity enable us to predict incipient cavitation for the pump. The flow rate divided by the inlet area gives the velocity perpendicular to the cascade, and the r.p.m. enables us to find the relative velocity parallel to the cascade. This relative velocity is in the opposite direction of the pump rotation. The vector sum of these two velocities determines the direction and magnitude of the inlet velocity to the cascade. Thus, we know V_i and γ_i, as shown in figure 5, and can determine the angle of attack from equation 20. The magnitude of (the velocity used in equation 18) is given by the equation

$$V^2 = V_i^2 + \left(\frac{\Gamma}{2S}\right)^2 - \frac{V_i \Gamma}{S} \cos \gamma_i$$

Having determined the angle of attack and the velocity, we can read the maximum velocity from the curves of figure 9. Cavitation occurs when the pressure in the fluid reaches its vapor pressure which is determined by the temperature. We can write the Bernoulli equation for the airfoil as follows:

$$\frac{P_0}{\rho} + \frac{1}{2} V_i^2 = \frac{P}{\rho} + \frac{1}{2} q^2$$

or

$$\sqrt{\frac{2(P_o - P)}{\rho} + V_i^2} = q$$

P_o is the static pressure ahead of the pump vanes in the inlet to the pump, V_i is the entering velocity relative to the pump vanes, and P is the vapor pressure. Since all these values are known, we can solve for q and from the curves, determine the angle of attack at which this value occurs. If it is the same or less than the angle of attack originally determined for V from the pump conditions, then cavitation will result. If it is larger than the angle of attack originally determined, then cavitation will not result. To find the exact point for incipient cavitation, we see that various flow rates and r.p.m. must be tried until the angle of attack determined by these two quantities is the same as the one read from the curve.

PART VI

FIGURES

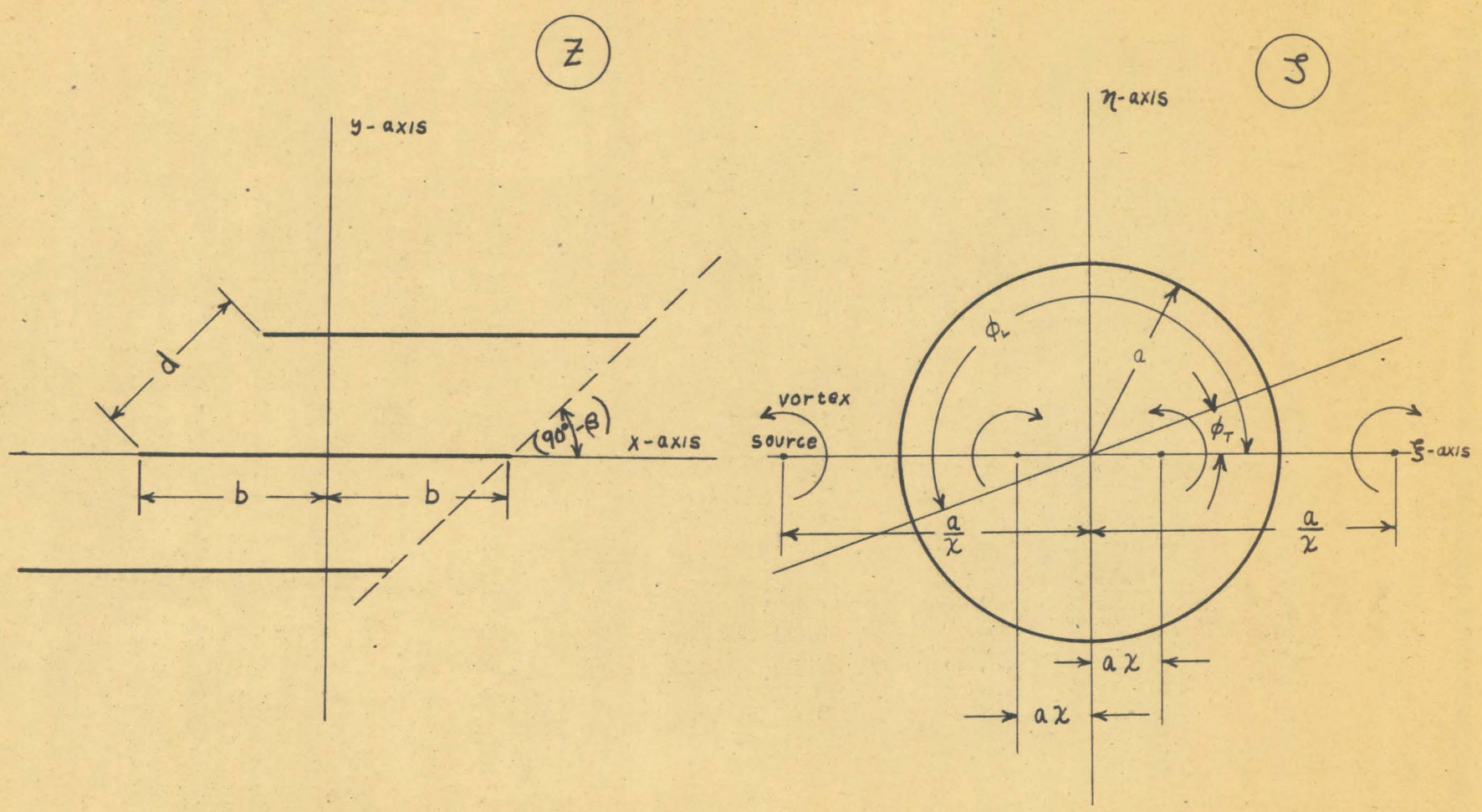

STRAIGHT LINE CASCADE TRANSFORMATION

FIGURE 1

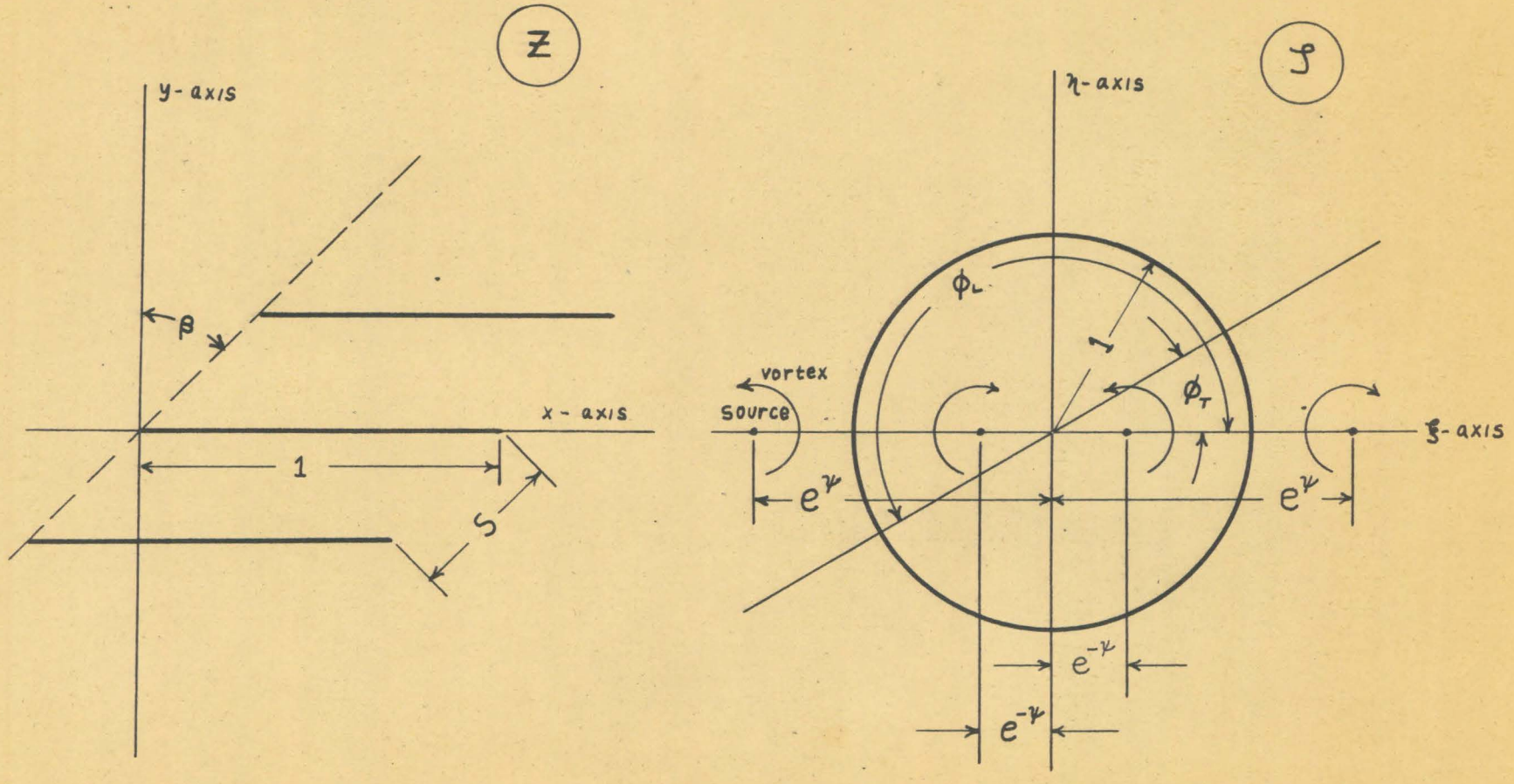

STRAIGHT LINE CASCADE TRANSFORMATION

FIGURE 2

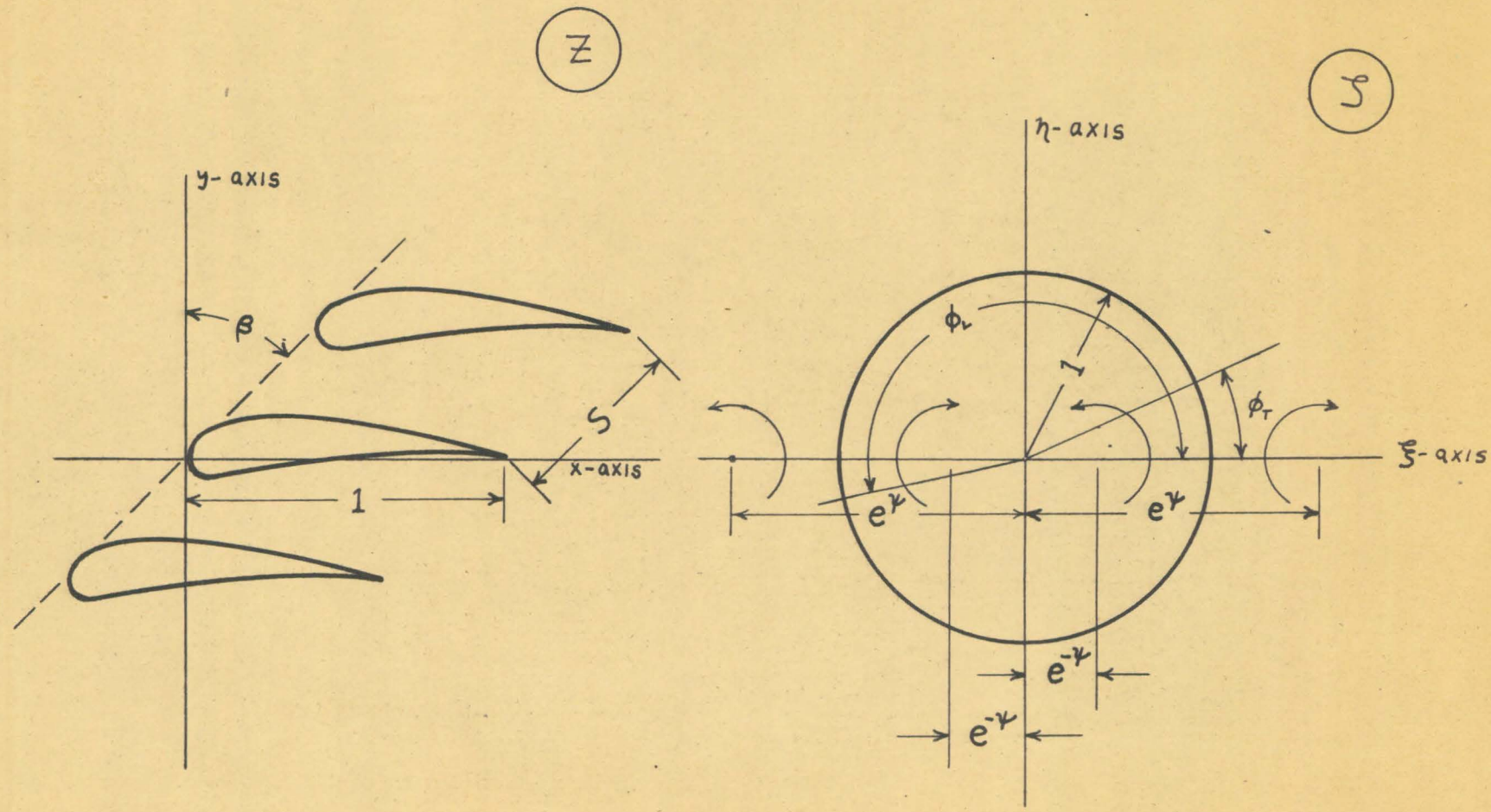

AIRFOIL CASCADE TRANSFORMATION

FIGURE 3

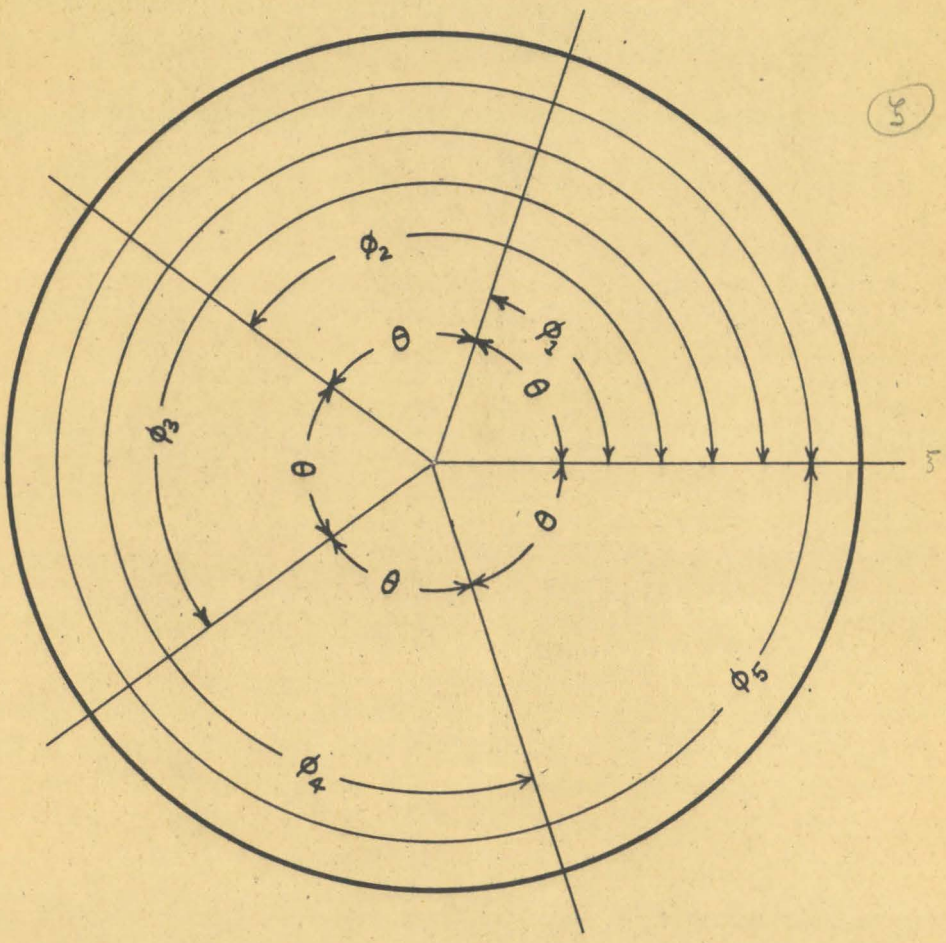

FIGURE 4

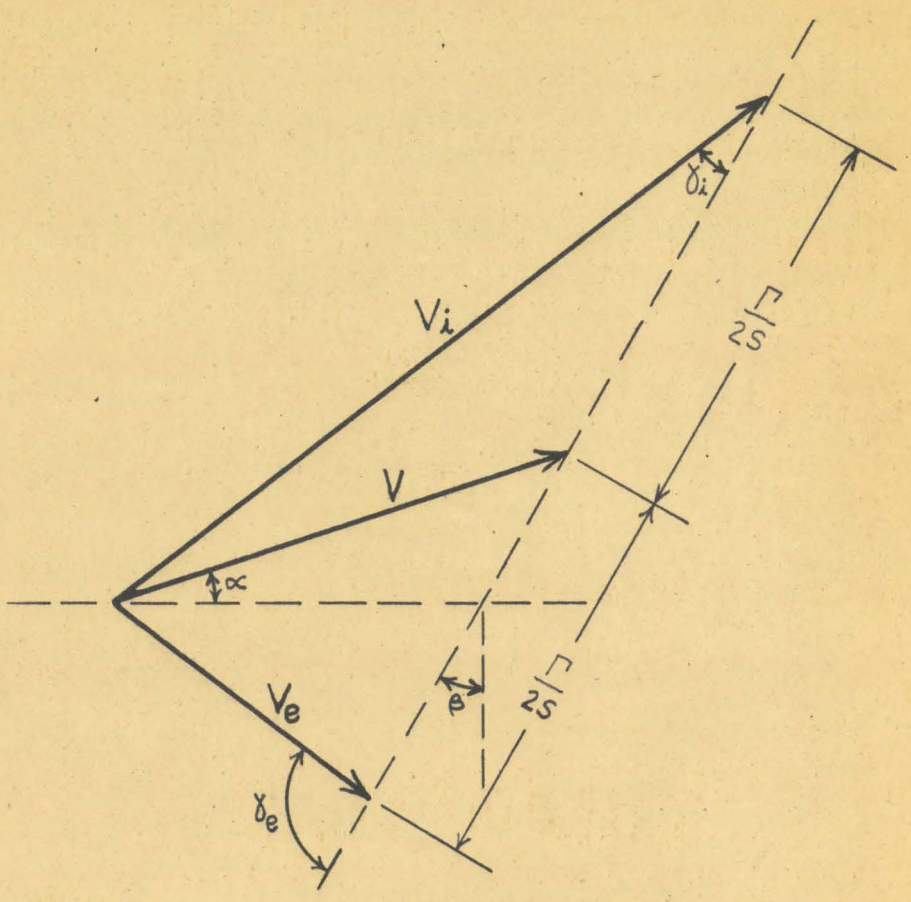

CASCADE VELOCITY DIAGRAM

FIGURE 5

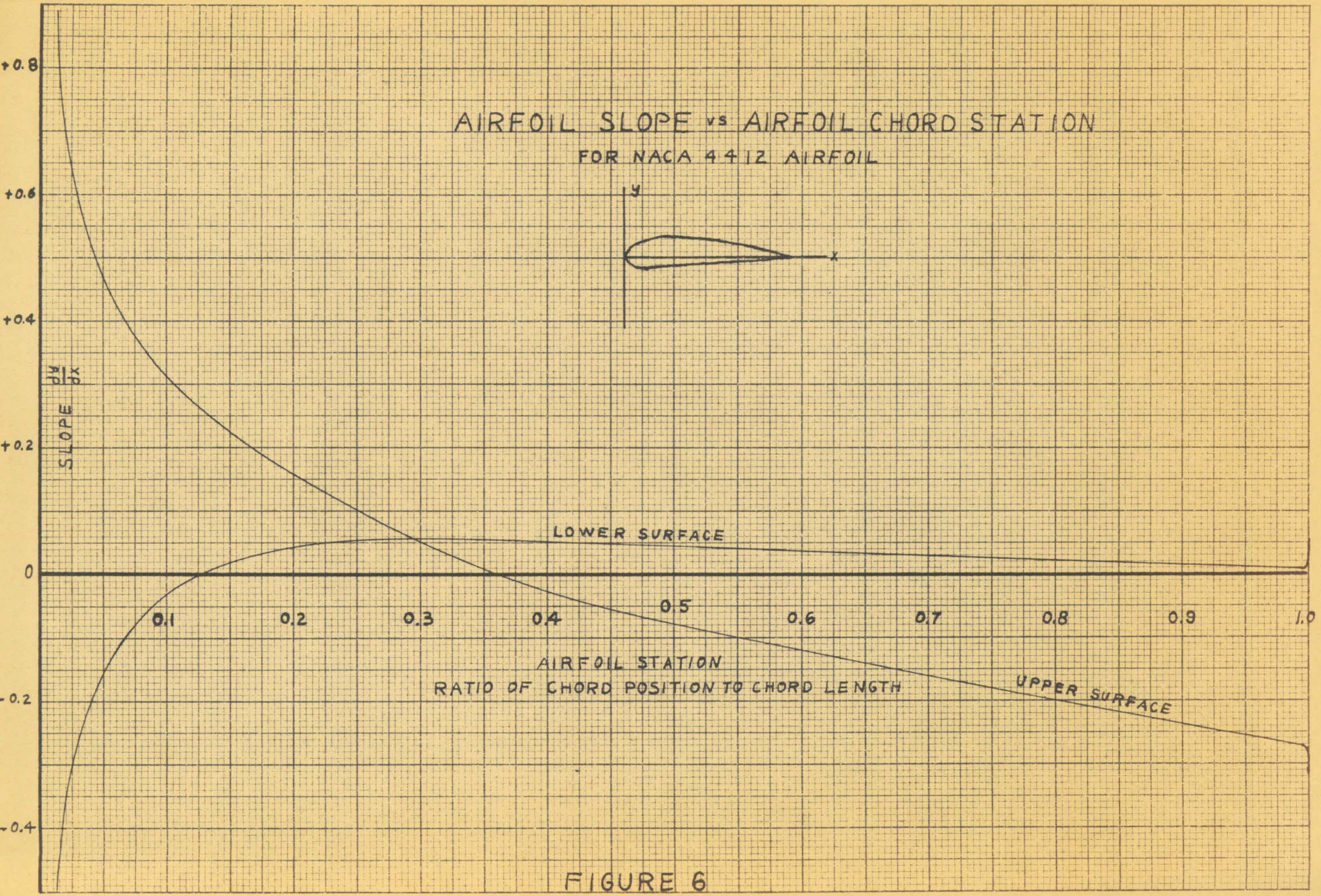
AIRFOIL SLOPE vs AIRFOIL CHORD STATION
FOR NACA 4412 AIRFOIL
y
x
+0.8
+0.6
+0.4
+0.2
0
-0.2
-0.4
SLOPE dy/dx
LOWER SURFACE
UPPER SURFACE
0.1
0.2
0.3
0.4
0.5
0.6
0.7
0.8
0.9
1.0
AIRFOIL STATION
RATIO OF CHORD POSITION TO CHORD LENGTH

FIGURE 6

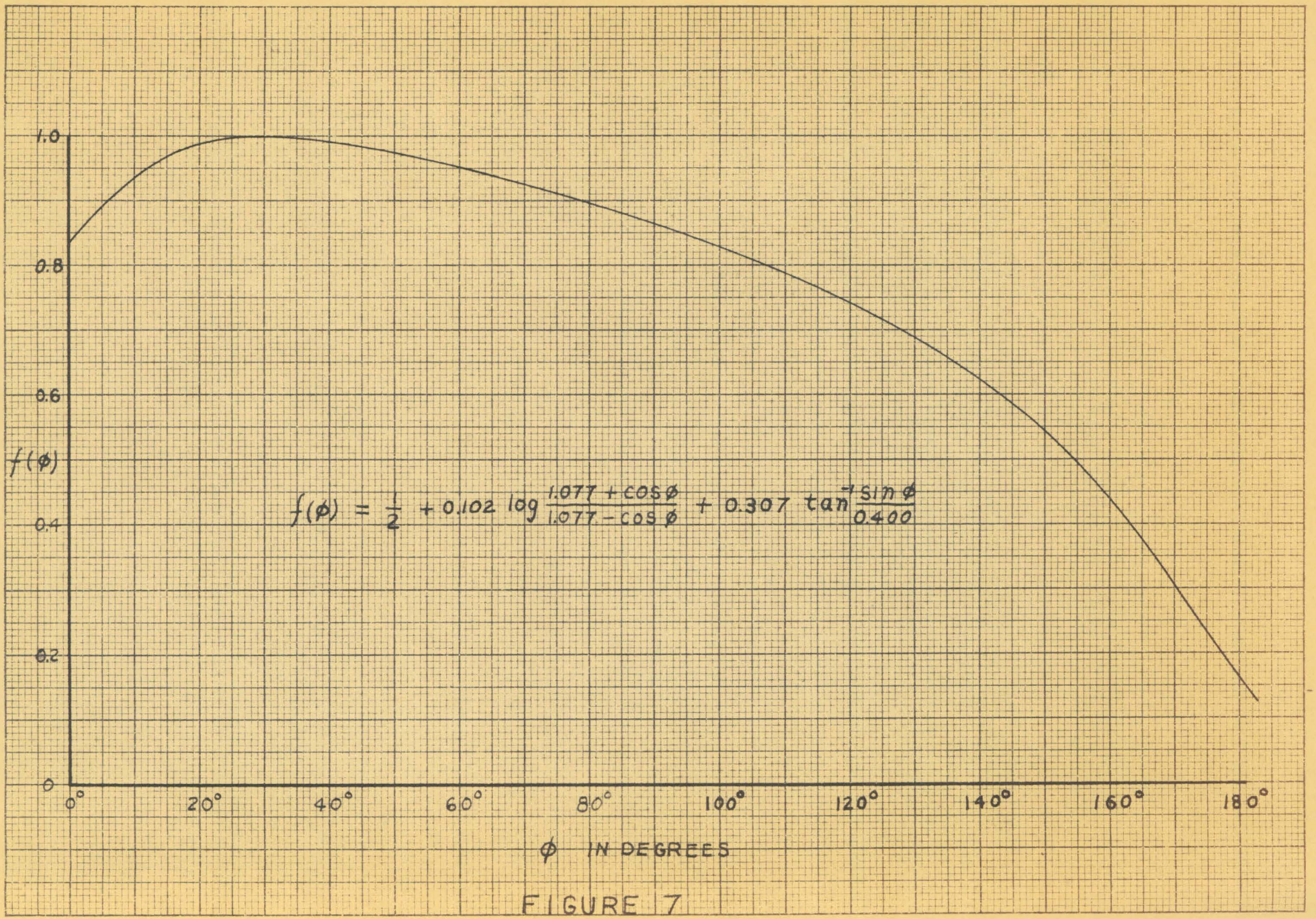
1.0
0.8
0.6
f(φ)
0.4
0.2
0
0°
20°
40°
60°
80°
100°
120°
140°
160°
180°
φ IN DEGREES
$f(\phi) = \frac{1}{2} + 0.102 \log \frac{1.077 + \cos\phi}{1.077 - \cos\phi} + 0.307 \tan^{-1} \frac{\sin\phi}{0.400}$

FIGURE 7

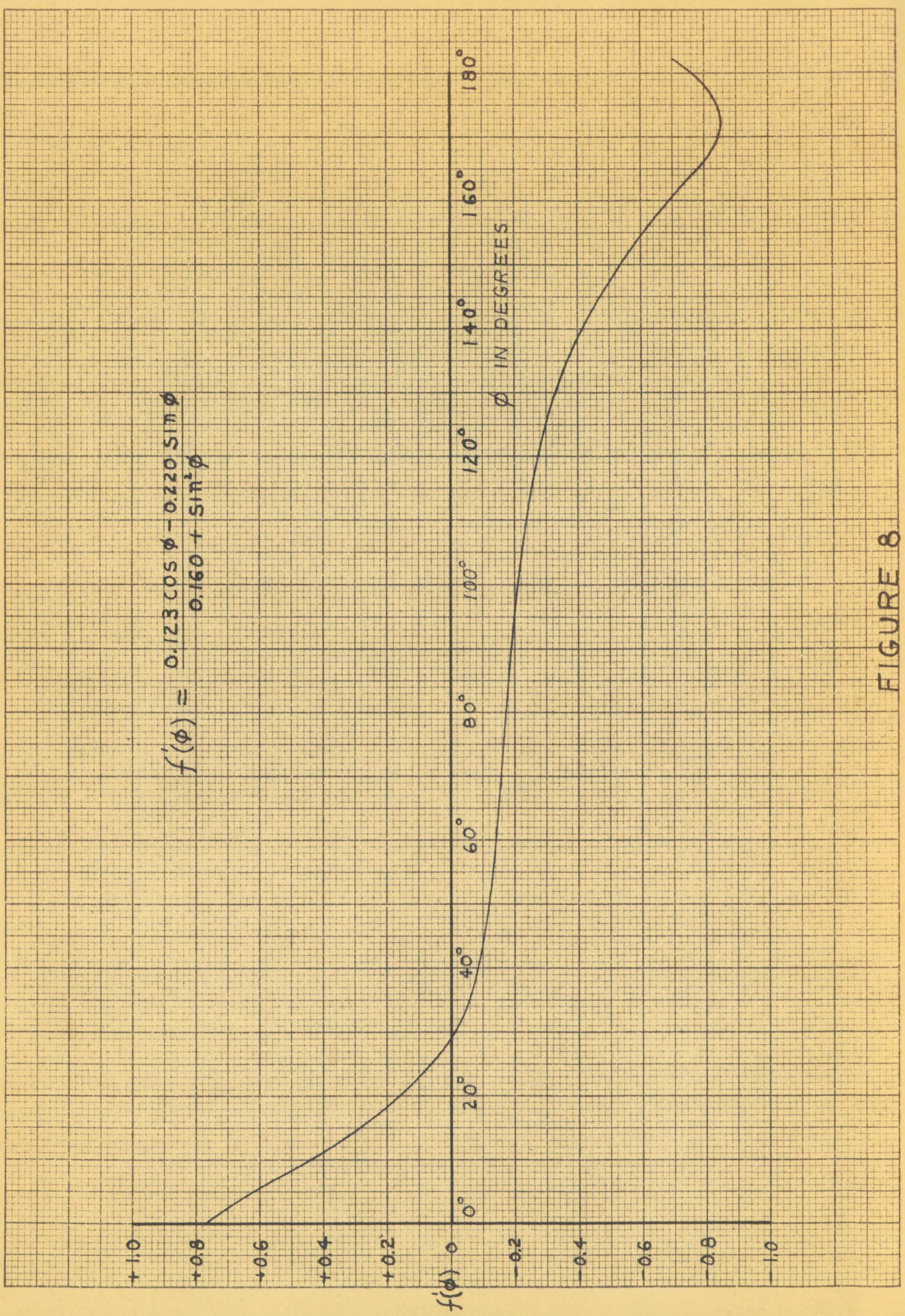
$f'(\phi) = \frac{0.123 \cos\phi - 0.220 \sin\phi}{0.160 + \sin^2\phi}$
+1.0
+0.8
+0.6
+0.4
+0.2
0
-0.2
-0.4
-0.6
-0.8
-1.0
f'(φ)
0°
20°
40°
60°
80°
100°
120°
140°
160°
180°
φ IN DEGREES

FIGURE 8

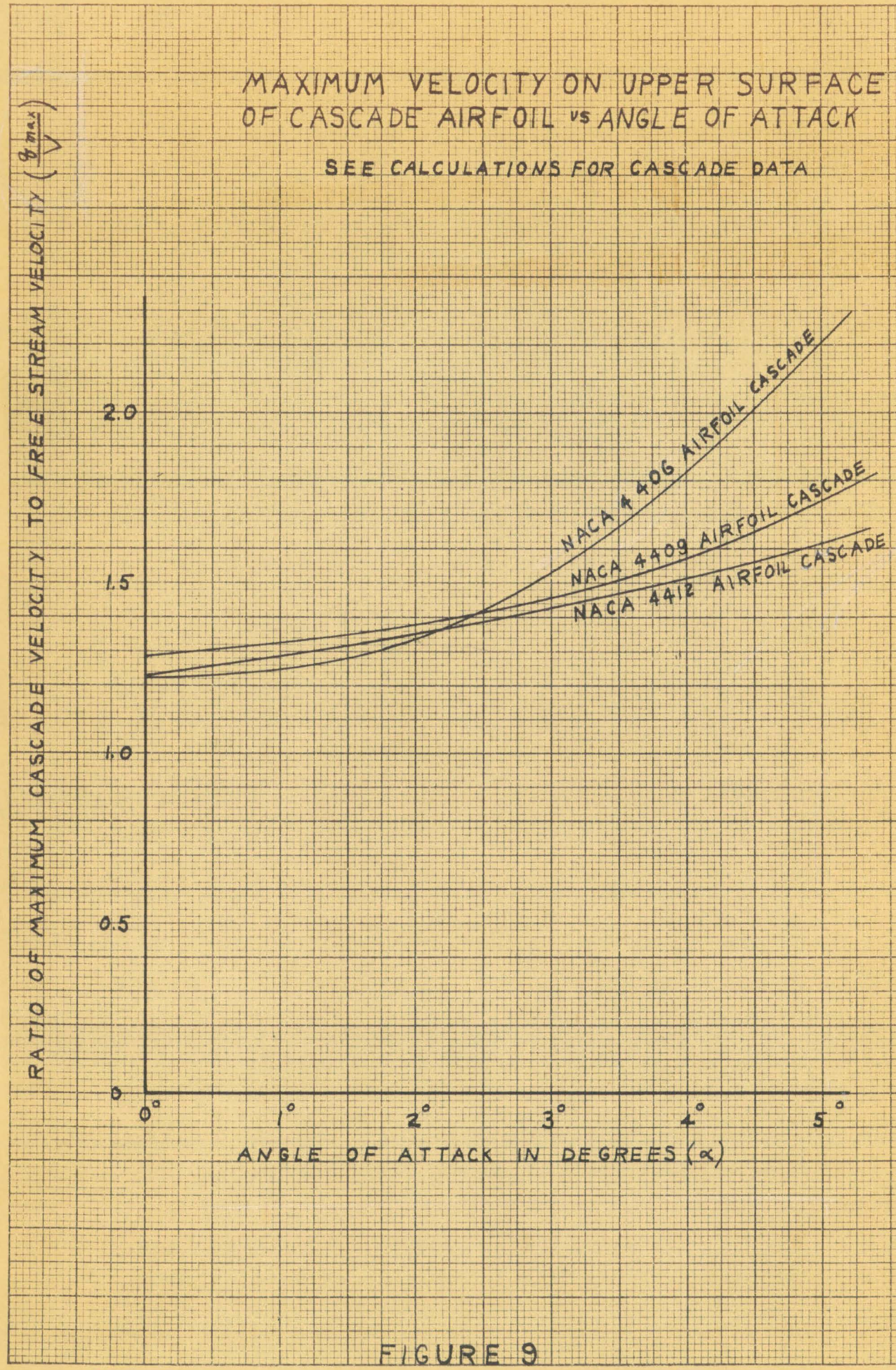
MAXIMUM VELOCITY ON UPPER SURFACE
OF CASCADE AIRFOIL vs ANGLE OF ATTACK
SEE CALCULATIONS FOR CASCADE DATA
RATIO OF MAXIMUM CASCADE VELOCITY TO FREE STREAM VELOCITY ($\frac{q_{max}}{V}$)
2.0
1.5
1.0
0.5
0
NACA 4406 AIRFOIL CASCADE
NACA 4409 AIRFOIL CASCADE
NACA 4412 AIRFOIL CASCADE
0°
1°
2°
3°
4°
5°
ANGLE OF ATTACK IN DEGREES (α)

FIGURE 9

VELOCITY DISTRIBUTION

ANGLE OF ATTACK = 0°
CASCADE AIRFOIL NACA 4412
GAP/CHORD = 1.16
CASCADE ANGLE = 56.4°

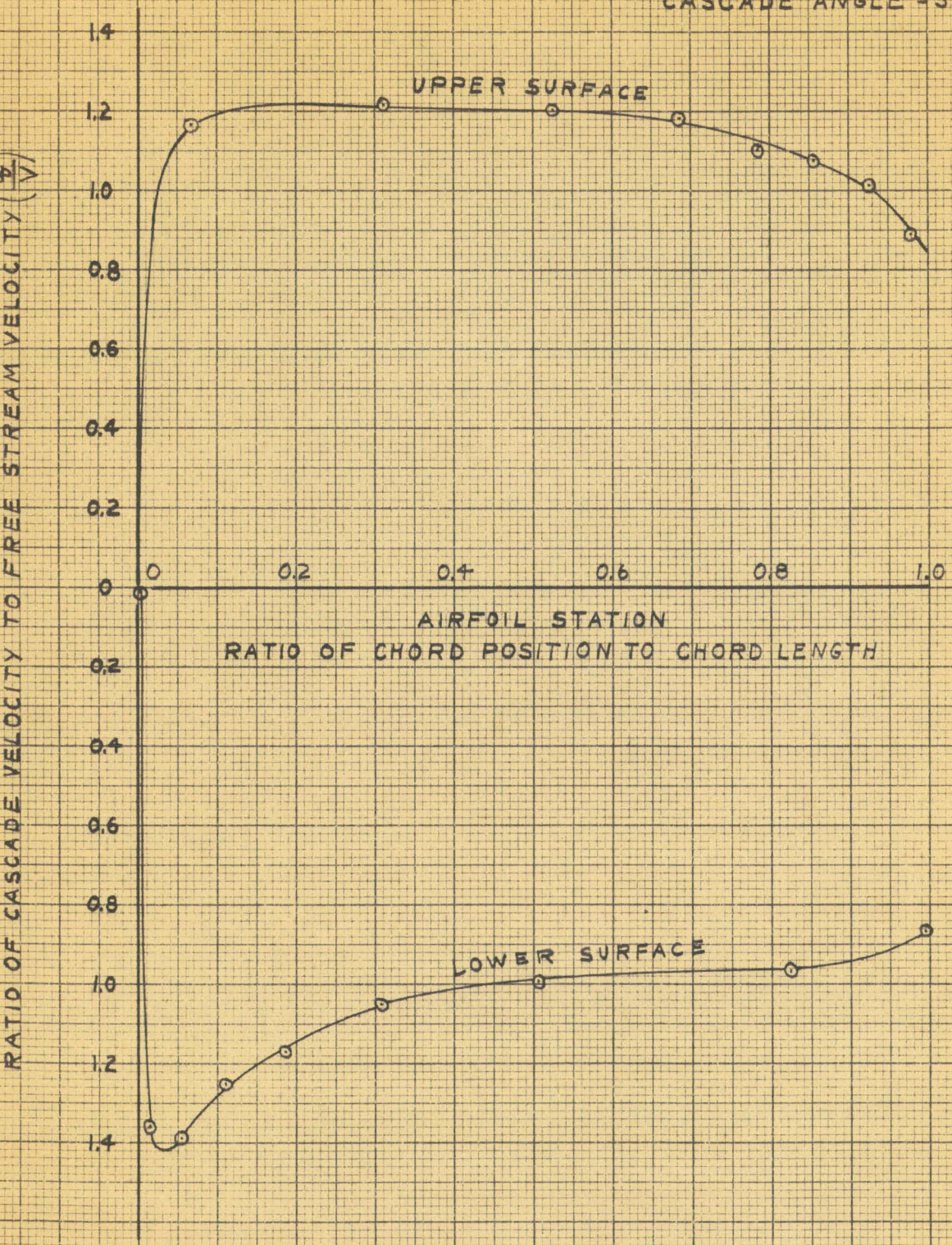

FIGURE 10

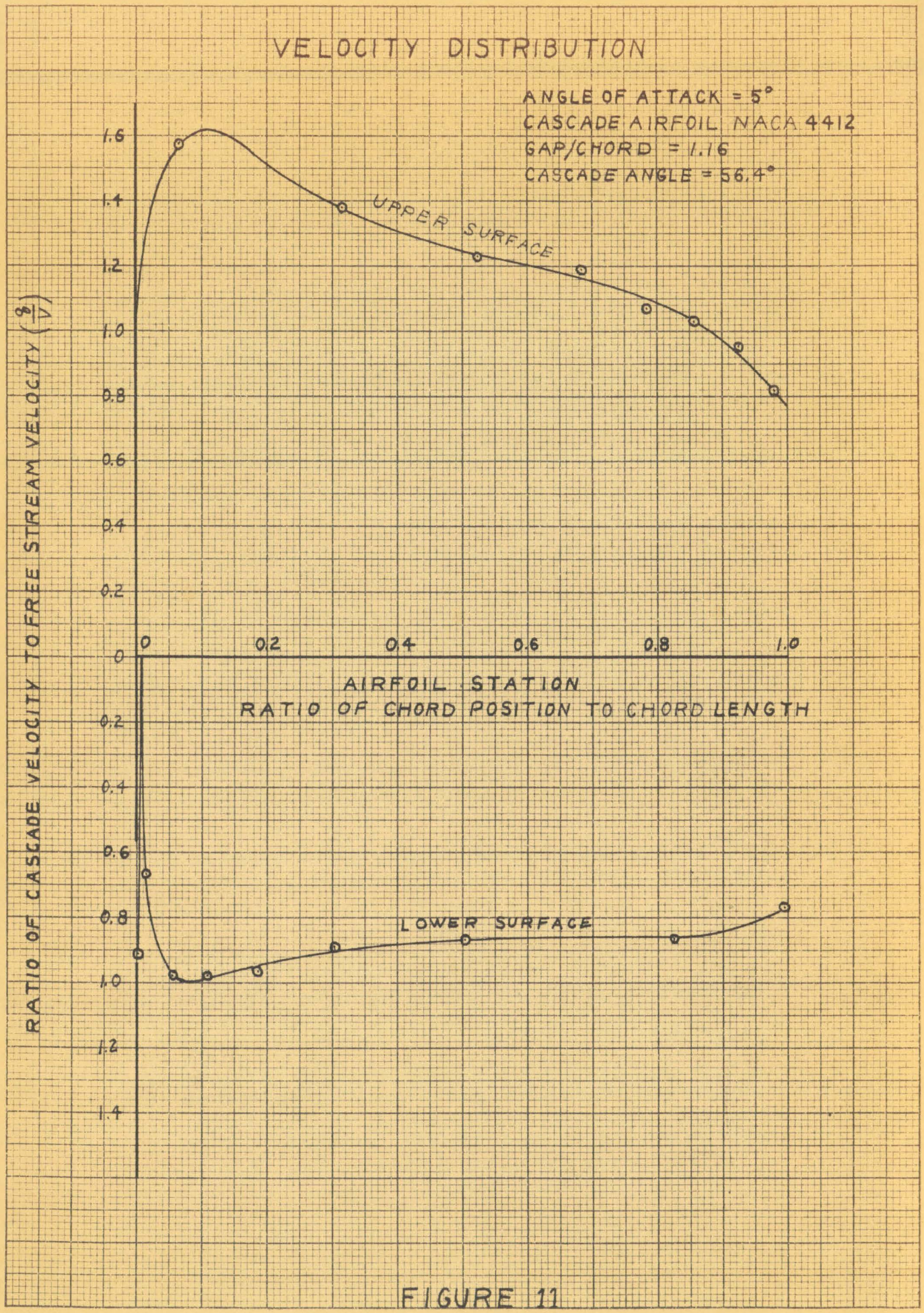
VELOCITY DISTRIBUTION
ANGLE OF ATTACK = 5°
CASCADE AIRFOIL NACA 4412
GAP/CHORD = 1.16
CASCADE ANGLE = 56.4°
UPPER SURFACE
LOWER SURFACE
RATIO OF CASCADE VELOCITY TO FREE STREAM VELOCITY (v/V)
AIRFOIL STATION
RATIO OF CHORD POSITION TO CHORD LENGTH
1.6
1.4
1.2
1.0
0.8
0.6
0.4
0.2
0
0.2
0.4
0.6
0.8
1.0
1.2
1.4
0
0.2
0.4
0.6
0.8
1.0

FIGURE 11

REFERENCES

1. S. Katzoff, R. S. Finn, and J. C. Laurence, "Interference Method for Obtaining the Potential Flow Past an Arbitrary Cascade of Airfoils,"NACA, T. N. 1254, May 1947.

2. F. Wdnig, "Die Strömung um die Schaufeln von Turbomaschinen", Johann Ambrosius Barth, (Leipzig), 1935.

3. T. Theodorsen, and I. E. Garrick, "General Potential Theory of Arbitrary Wing Sections," NACA Report 452, 1933.

4. I. E. Garrick, "On the Plane Potential Flow Past a Lattice of Arbitrary Airfoils," NACA, ARR 4A07, January 1944.

5. W. Mutterperl, "A Solution of the Direct and Inverse Potential Problems for Arbitrary Cascades of Airfoils," NACA, A.R.R. L4K22b, December 1944.

6. A. R. Howell, "Note on the Theory of Arbitrary Aerofoils in Cascade," RAE Note E. 3859, March 1941.

7. A. W. Goldstein, and M. Jerison, "Isolated and Cascade Airfoils with Prescribed Velocity Distribution," NACA, TN 1308, May 1947.

8. L. Diesendruck, "Iterative Interference Methods in the Design of Thin Cascade Blades," NACA, T.N. 1254, May 1947.

9. W. F. Durand, "Aerodynamic Theory," California Institute of Technology, Pasadena, California, Vol. II, 1943, p. 93,94.

10. Karl Stumpff, "Tafeln und Aufgaben Zur Harmonischen Analyse und Periodogrammrechnung," Springer, 1939, reprinted by J. W. Edwards, Ann Arbor, Michigan, 1944.

11. Eastman N. Jacobs, Kenneth E. Ward, and Robert M. Pinkerton, "Characteristic of 78 Related Airfoil Sections from Tests in the Variable-density Wind Tunnel," NACA, T.R. #460, 1933.

12. George F. Wislicenus, "Fluid Mechanics of Turbomachinery," McGraw-Hill Book Company, Inc., New York, 1947.

BIBLIOGRAPHY IN ADDITION TO REFERENCES

1. A. D. S. Carter and H. P. Hughes, "A Theoretical Investigation into the Effect of Profile Shape on the Performance of Aerofoils in Cascade," Power Jets Report, R1192, April 1947.

2. A. R. Collar, "Cascade Theory and the Design of Fan Straightoners," British A. R. C., R. & M. 1885, January 1940.

3. A. R. Collar, "The Flow of a Perfect Fluid Through Cascades of Aerofoils," Roy. Aero. Soc., Vol. XLV, No. 365, May 1941.

4. J. C. Hunsaker and B. G. Rightmire, "Engineering Applications of Fluid Mechanics," McGraw-Hill Book Company, 1947.

5. Sir Horace Lamb, "Hydrodynamics," Dover Publications, New York, 1945.

6. W. Merchant and A. R. Collar, "Flow of Ideal Fluid Past a Cascade of Blades." British A. R. C., R. & M. 1893, May 1941.

7. W. Merchant and J. T. Hansford, "Flow of an Ideal Fluid Through a Cascade of Blades," (Summary Report) Metropolitan Vickers Report, June 1945.

8. W. D. Rannie, "On the Calculations of Velocity Distributions for Single Airfoils and Airfoils in Cascades," unpublished report.

9. R. A. Spurr, H. Julian Allen, "A Theory of Unstaggered Airfoil Cascades in Compressible Flow," NACA, R.M. A7E29, September 1947.

10. F. Wenig, "Strömung Durch Profilgitter und Einige Anwendungen auf die Strömung in Propellern," Hydromechanische Probleme des Schiffsantriebs, 1932, p. 171.

APPENDIX A

A proposed method of summing

$$\frac{dy}{d\phi} = \sum_{n=0}^{\infty} -n B_n \sin(n\phi) + \sum_{n=0}^{\infty} -n A_n \cos(n\phi)$$

Divide the circle into N (odd) sections and determine $\frac{dy}{d\phi}$ at each of these points, letting

$$Y_0 = \left(\frac{dy}{d\phi}\right)_{\phi=0}, \quad Y_1 = \left(\frac{dy}{d\phi}\right)_{\phi=\frac{2\pi}{N}}, \quad \cdots\cdots, \quad Y_{N-1} = \left(\frac{dy}{d\phi}\right)_{\phi=\frac{4P\pi}{N}} \quad (N=2P+1)$$

Then, we have

$$\left.\begin{aligned} -\frac{\mu N A_\mu}{2} &= \sum_{j=0}^{j=N-1} Y_j \cos(\mu j\theta) \\ -\frac{\mu N B_\mu}{2} &= \sum_{j=0}^{j=N-1} Y_j \sin(\mu j\theta) \end{aligned}\right\} \quad \begin{aligned} &\theta = \frac{2\pi}{N} \\ &\phi_j = j\theta \\ &\mu = 1, 2, \cdots\cdots, P \end{aligned}$$

Let $C_0 = Y_0$, $C_1 = Y_1 + Y_{N-1}$, $C_2 = Y_2 + Y_{N-2}$, $\cdots\cdots$, $C_\nu = Y_\nu + Y_{N-1-\nu}$

and $S_1 = Y_1 - Y_{N-1}$, $S_2 = Y_2 - Y_{N-2}$, $\cdots\cdots\cdots$, $S_\nu = Y_\nu - Y_{N-1-\nu}$ $\left(\nu = 0, 1, 2, \cdots, \frac{N-1}{2}\right)$

Using these values as shown, we obtain the following tables given for 11 and 17 divisions.

TABLE I (N=11)

j	jθ	|cosjθ|	sinjθ	μ=1 C_ν S_ν	μ=2 C_ν S_ν	μ=3 C_ν S_ν	μ=4 C_ν S_ν	μ=5 C_ν S_ν
0	0°	1.000		0 -	0 -	0 -	0 -	0 -
1	32.73°	0.841	0.541	1 1	5 -5	4 4	3 3	2 -2
2	65.45°	0.415	0.910	2 2	1 1	3 -3	5 -5	4 -4
3	98.18°	0.142	0.990	-3 3	-4 -4	-1 1	-2 -2	-5 5
4	130.91°	0.655	0.756	-4 4	-2 2	-5 5	-1 1	-3 3
5	163.64°	0.959	0.282	-5 5	-3 -3	-2 -2	-4 4	-1 1

TABLE II (N=17)

j	jθ	|cos jθ|	sin jθ	μ=1 C_{ν} S_{ν}	μ=2 C_{ν} S_{ν}	μ=3 C_{ν} S_{ν}	μ=4 C_{ν} S_{ν}	μ=5 C_{ν} S_{ν}	μ=6 C_{ν} S_{ν}	μ=7 C_{ν} S_{ν}	μ=8 C_{ν} S_{ν}
0	0°	1.000		0 -	0 -	0 -	0 -	0 -	0 -	0 -	0 -
1	21.18°	0.932	0.361	1 1	8 -8	6 6	4 -4	7 7	3 3	5 5	2 -2
2	42.35°	0.739	0.674	2 2	1 1	5 -5	8 -8	3 -3	6 6	7 -7	4 -4
3	68.53°	0.446	0.895	3 3	7 -7	1 1	5 5	4 4	8 -8	2 -2	6 -6
4	84.71°	0.092	0.996	4 4	2 2	7 7	1 1	6 -6	5 -5	3 3	8 -8
5	105.88°	0.274	0.962	-5 5	-6 -6	-4 -4	-3 -3	-1 1	-2 -2	-8 8	-7 7
6	127.06°	0.603	0.798	-6 6	-3 3	-2 2	-7 -7	-8 8	-1 1	-4 -4	-5 5
7	148.24°	0.850	0.526	-7 7	-5 -5	-8 8	-6 6	-2 -2	-4 4	-1 1	-3 3
8	169.41°	0.983	0.184	-8 8	-4 4	-3 -3	-2 2	-5 5	-7 7	-6 6	-1 1

For example, with $N = 11$ $\mu = 3$

$$-\frac{3(11)A_3}{2} = C_0 + 0.841C_4 + 0.415C_3 - 0.142C_1 - 0.655C_5 - 0.959C_2$$

$$-\frac{3(11)B_3}{2} = 0.541S_4 - 0.910S_3 + 0.990S_1 + 0.756S_5 - 0.282S_2$$